

*Review*  
File Copy

SOME ANALYTICAL AND PRACTICAL ASPECTS  
OF WIENER'S THEORY OF PREDICTION

ROBERT COHEN

TECHNICAL REPORT NO. 69

JUNE 2, 1948

RESEARCH LABORATORY OF ELECTRONICS  
MASSACHUSETTS INSTITUTE OF TECHNOLOGY

The research reported in this document was made possible through support extended the Massachusetts Institute of Technology, Research Laboratory of Electronics, jointly by the Army Signal Corps, the Navy Department (Office of Naval Research), and the Air Force (Air Materiel Command), under the Signal Corps Contract No. W-36-039 sc-32037.

MASSACHUSETTS INSTITUTE OF TECHNOLOGY  
Research Laboratory of Electronics

Technical Report No. 69

June 2, 1948

SOME ANALYTICAL AND PRACTICAL ASPECTS  
OF WIENER'S THEORY OF PREDICTION\*

---

\* This report is a copy of a thesis with the same title submitted by the author in partial fulfillment of the requirements for the degree of Master of Science in Electrical Engineering at the Massachusetts Institute of Technology, May, 1948.



## ABSTRACT

The performance of the Wiener predictor is shown to be closely connected to the behavior of the signal derivatives; in turn, this behavior is related to the structure of the signal autocorrelation curve in the immediate vicinity of the ordinate axis. Careful reproduction of this structure in the analytical work is the fundamental condition for an accurate predictor design. The expected performance of the predictor, measured by the "error", may be anticipated by noticing that: (a) a signal whose first derivative reaches infinite values is practically unpredictable; (b) prediction is possible if at least the first derivative of the signal remains finite; and (c) the quality of prediction increases when derivatives of increasing orders of the signal are constrained to remain finite. Again, these characteristics of the signal derivatives are interpreted in the central structure of the autocorrelation curve. For example, a common feature of "predictable" signals is that their autocorrelation curves have zero initial slopes.

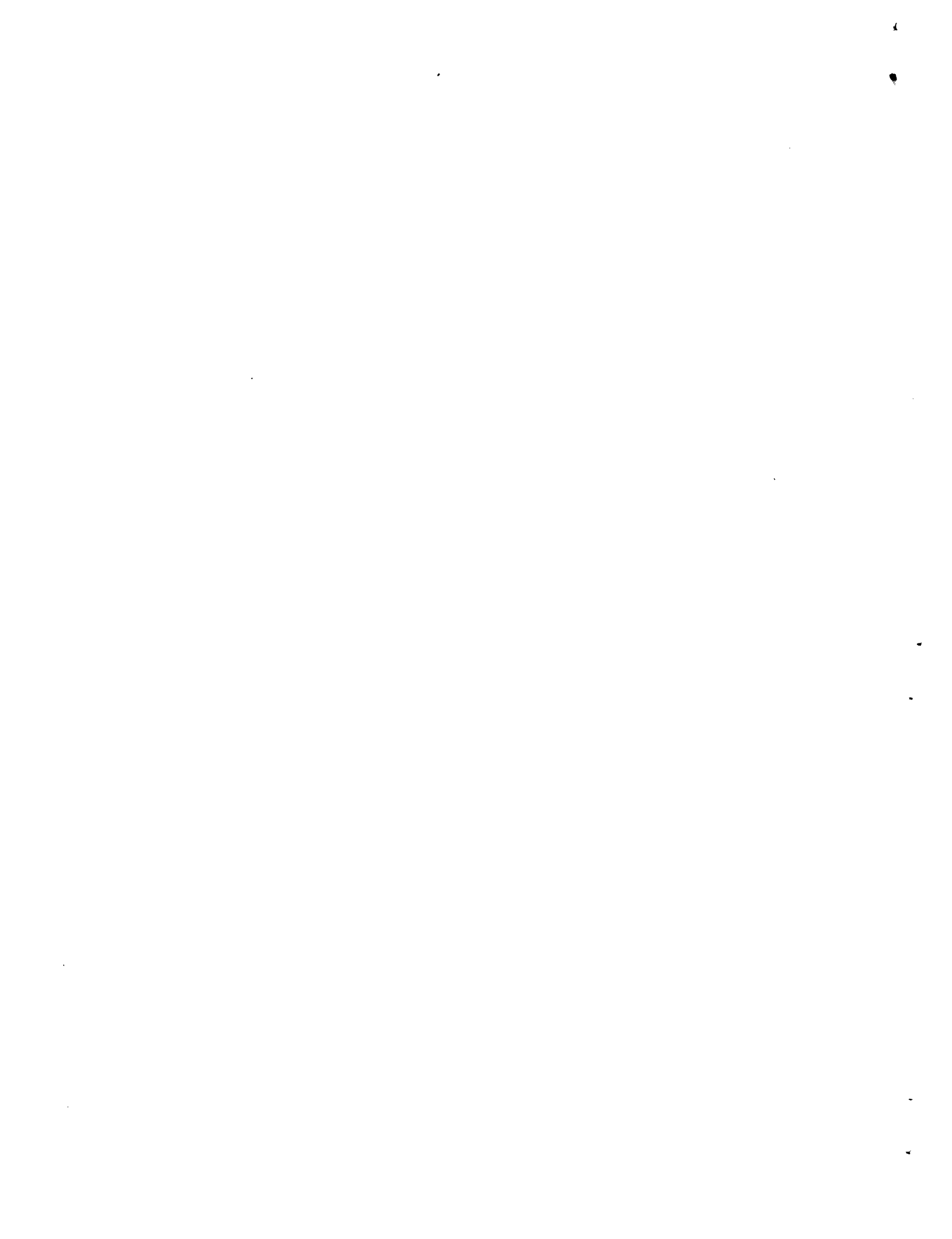
Failure to give due weight to the severe accuracy requirements in fitting analytically the central part of the autocorrelation curve accounts for the unsatisfactory results obtained in a first trial experiment on prediction, attempted in Chapter II.

A close correspondence between the central region of the autocorrelation curve and the high frequency content of the signal is recognized. If one deals with experimental data on power spectrum, it follows that the higher the frequency range, the greater the required accuracy of the data for prediction analysis. In all prediction experiments it is therefore more adequate to deal with autocorrelation data, which need to be accurately reproduced only in a narrow range of the variable. The analytical expression thus obtained for the autocorrelation curve gives the power spectrum by a simple Fourier transformation.

## TABLE OF CONTENTS

	Page
CHAPTER I. INTRODUCTION .....	1
1. Generalities .....	1
2. Brief Historical Background .....	7
3. Purpose of the Present Paper .....	8
CHAPTER II. A TRIAL EXPERIMENT ON PREDICTION .....	10
1. Choice of the Input Function .....	10
2. Experimental Computation of Autocorrelation Function ..	13
3. Functional Approximation to Experimental Autocorrelation .....	18
4. Optimum Predictor System Function .....	25
5. Performance of the Predictor Operator .....	27
CHAPTER III. STRUCTURAL RELATIONS BETWEEN TIME FUNCTION AND AUTOCORRELATION CURVE .....	30
1. Fundamental Theorems .....	30
Theorem I .....	30
Theorem II .....	31
Theorem III .....	33
Theorem IV .....	35
Theorem V .....	37
Theorem VI .....	45
2. Smooth Time Functions .....	49
3. Jump Time Functions .....	50

	Page
CHAPTER IV. THE POWER SPECTRUM FUNCTION .....	51
1. Separation of Conjugate Singularities .....	51
2. Differentiation .....	53
CHAPTER V. A STUDY OF PREDICTION ERROR IN RELATION TO SIGNAL AND AUTOCORRELATION BEHAVIOR .....	58
1. The Unit-Transfer-Error Curve .....	58
2. The Zero-Transfer-Error Curve .....	60
3. Behavior of the Wiener Prediction Error for Large $\alpha$ .....	61
4. Behavior of the Wiener Prediction Error for Small $\alpha$ .....	62
5. Examples .....	69
6. The Relative Error in Prediction .....	77
CHAPTER VI. CONCLUSIONS .....	82
APPENDIX I .....	88
APPENDIX II .....	89
APPENDIX III .....	90
APPENDIX IV .....	94
APPENDIX V .....	97
ACKNOWLEDGMENTS .....	99
BIBLIOGRAPHY .....	100





## CHAPTER I

### Introduction

#### 1. Generalities

The filter problem, in communication engineering, may be defined as the problem of recovering a given signal, selected among a number of other signals or disturbances that may be present.

The classical solution given to this problem consists in conveying the various signals through separate frequency "channels," and designing filter systems, each responding to the desired channel, with as sharp as possible a "cut-off" in amplitude response, in order to prevent overlapping of the frequency ranges assigned to the other signals.

The sharp cut-off in the amplitude response is unfortunately associated with a strong distortion in the phase response.

The ear seems to tolerate a considerable amount of phase distortion, which therefore results in a minor disadvantage in the reproduction of audible signals. But when the ultimate destination of the signal is either the eye, as in the video reproduction of television receivers, or a mechanical system driven by a servomechanical transmission, then phase distortion may become seriously inconvenient.

Another disadvantage of the classical solution lies in the fact that it disregards such random disturbances known as "noise," whose interference into the frequency channel considered cannot be completely discriminated against.

On account of these difficulties, a completely new approach to the general filter problem has been given by N. Wiener in an NDRC Report dated February 1, 1942,<sup>1</sup> and made public in 1945.

Under this approach, signals are considered in the time domain to begin with, and as such are recognized as effectively covering the entire frequency range when transposed into the frequency domain. Whereas the classical solution focussed attention upon the response to sinusoidal time signals confined within the region surrounding the carrier frequency, Wiener attempted to deal with the actual signal and the statistical character of its time representation.

A fundamental requirement for studying the problem along these lines is that the signals considered must represent stationary time series. In other words, their individual statistical properties must be fixed in time. It is intuitively evident that such conditions are met, for example, in the time representation of speech messages modulating some arbitrary carrier frequency: Speaking of stationary statistical characteristics for such messages amounts to saying that, in a given language, the frequency of occurrence of any letter of the alphabet is governed by a fixed probability distribution pattern; and the succession of letters, associating any one of them with the others, gives rise to combinations which follow statistical laws.

Under such conditions we may say that if we split the message into its sinusoidal Fourier components, we shall find components having a certain distribution in relative amplitude and phase, characterizing the statistical properties of the message considered. Whereas the classical approach considers these sinusoidal components individually,

disregarding the manner in which they contribute to the actual message, Wiener has shown that the optimum solution to the filter problem is obtained by choosing a convenient measure of the distribution of these components. This measure is the power spectrum, representing the average power density of the message for any frequency component. Alternatively, an equivalent representation of the statistics of the message is given by its autocorrelation function  $\varphi_{11}(\tau)$ , defined as:<sup>2</sup>

$$\varphi_{11}(\tau) = \lim_{T \rightarrow \infty} \frac{1}{2T} \int_{-T}^T f_1(t) f_1(t + \tau) dt, \quad (1)$$

where  $f_1(t)$  is the time representation of the message.

The equivalence between autocorrelation  $\varphi_{11}(\tau)$  and power spectrum  $\Phi_{11}(\omega)$  lies in the fact that they are Fourier transforms of one another.<sup>3</sup>

Symbolically,

$$\Phi_{11}(\omega) = \frac{1}{2\pi} \int_{-\infty}^{\infty} \varphi_{11}(\tau) e^{-j\omega\tau} d\tau, \quad (2)$$

$$\varphi_{11}(\tau) = \int_{-\infty}^{\infty} \Phi_{11}(\omega) e^{j\omega\tau} d\omega. \quad (3)$$

When two signals  $f_1(t)$  and  $f_2(t)$  are present, "cross-correlation" terms may arise, and lead to analogous definitions:

$$\varphi_{12}(\tau) = \lim_{T \rightarrow \infty} \frac{1}{2T} \int_{-T}^T f_1(t) f_2(t + \tau) dt, \quad (4)$$

$$\Phi_{12}(\omega) = \frac{1}{2\pi} \int_{-\infty}^{\infty} \varphi_{12}(\tau) e^{-j\omega\tau} d\tau, \quad (5)$$

$$\varphi_{12}(\tau) = \int_{-\infty}^{\infty} \Phi_{12}(\omega) e^{j\omega\tau} d\omega \quad (6)$$

These "cross-terms" are identically zero or constants if the two signals considered are incoherent; for example, a speech message and "shot noise" produced by an amplifier are completely unrelated, and their cross-correlation is zero.

One particular problem whose solution is given by Wiener's theory in terms of the symbols defined above is the following: Consider a signal  $f_1(t)$  and an interfering signal  $f_2(t)$ ; the expression

$$f_i(t) = f_1(t) + f_2(t) \quad (7)$$

represents the "corrupted" signal that we are confronted with, and that we apply at the input terminals of a filter. What is the optimum filter transfer function (or "system" function) in order that, under such conditions, the filter output  $f_o(t)$  reproduce "as closely as possible" the "uncorrupted" signal  $f_1$ ? The criterion of performance chosen by Wiener is that the transfer function should be so chosen that it minimizes the "mean-square error" between observed and expected outputs. Formally, it must minimize the expression:

$$\varepsilon = \lim_{T \rightarrow \infty} \frac{1}{2T} \int_{-T}^T \left[ f_o(t) - f_1(t - \alpha) \right]^2 dt, \quad (8)$$

where  $\alpha$  represents a fixed lag or time delay after which the signal  $f_1(t)$  is expected to be approximated by the output  $f_o(t)$ . The formal solution to the minimization problem has the remarkable property of being independent of the algebraic sign attached to the parameter  $\alpha$ ; in other words, a "predictor" may be synthesized as a particular case

of a filter having a leading time response. To emphasize the generality of the solution, the parameter is written as  $\pm \alpha$ . In terms of the complex frequency variable

$$\lambda = \omega + j\sigma \quad (9)$$

the transfer function resulting from Wiener's analysis reads:

$$H(\lambda) = \frac{1}{2\pi \Phi_{ii}^+(\lambda)} \int_0^{\infty} \Psi(t \pm \alpha) e^{-j\lambda t} dt, \quad (10)$$

where

$$\Psi(t \pm \alpha) = \int_{-\infty}^{\infty} \frac{\Phi_{11}(\omega) + \Phi_{12}(\omega)}{\Phi_{ii}^-(\omega)} e^{j(t \pm \alpha)\omega} d\omega \quad (11)$$

In these expressions, the "input power spectrum"

$$\Phi_{ii} = \Phi_{11} + \Phi_{22} + 2\Phi_{12} \quad (12)$$

is "factorized" into product components  $\Phi_{ii}^+$  and  $\Phi_{ii}^-$  containing, respectively, those poles and zeros of  $\Phi_{ii}$  that lie in the upper and the lower half of the complex frequency variable plane. We have:

$$\Phi_{ii} = \Phi_{ii}^+ \Phi_{ii}^- \quad (13)$$

System function (10) minimizes the mean-square error (8) between the observed output  $f_o(t)$  and the uncorrupted signal  $f_1(t \pm \alpha)$ .

This error, however, is not zero; its value is given by:

$$\epsilon_{\min} = \varphi_{11}(0) - \frac{1}{2\pi} \int_0^{\infty} \Psi^2(t \pm \alpha) dt \quad (14)$$

In a great number of problems, the signals in presence,  $f_1(t)$  and  $f_2(t)$  are incoherent; for example,  $f_1(t)$  may be a speech message and  $f_2(t)$  shot noise. Then  $\Phi_{12} = 0$  and eqs. 11 and 12 become:

$$\Psi(t \pm \alpha) = \int_{-\infty}^{\infty} \frac{\Phi_{11}^+(\omega)}{\Phi_{ii}^-(\omega)} e^{j(t \pm \alpha)\omega} d\omega, \quad (15)$$

$$\Phi_{ii}(\omega) = \Phi_{11}(\omega) + \Phi_{22}(\omega). \quad (16)$$

A particular problem, with which this paper will be mainly concerned, is the one of "pure prediction," in which  $f_2(t)$  is made equal to zero in order to optimize the performance. The function of the filter, or "pure predictor," is then to extrapolate the message  $f_1(t)$  into the future, message statistics being described by its power spectrum.

In this case,  $\Phi_{ii} = \Phi_{11}$ ;  $\frac{\Phi_{11}}{\Phi_{ii}^-} = \Phi_{11}^+$ . Symbols and equations defined above read as follows, for the case of a single message

function  $f(t)$ :

$$\varphi(\tau) = \varphi_{ff}(\tau) = \lim_{T \rightarrow \infty} \frac{1}{2T} \int_{-T}^T f(t) f(t + \tau) dt, \quad (17)$$

$$\varphi(\tau) = \int_{-\infty}^{\infty} \Phi(\omega) e^{j\omega\tau} d\omega, \quad (18)$$

$$\Phi(\omega) = \frac{1}{2\pi} \int_{-\infty}^{\infty} \varphi(\tau) e^{-j\omega\tau} d\tau = \Phi^+(\omega) \Phi^-(\omega), \quad (19)$$

$$H(\lambda) = \frac{1}{2\pi \Phi^+(\lambda)} \int_0^{\infty} \Psi(t + \alpha) e^{-j\lambda t} dt, \quad (20)$$

$$\Psi(t + \alpha) = \int_{-\infty}^{\infty} \Phi^+(\omega) e^{j(t+\alpha)\omega} d\omega. \quad (21)$$

If  $f_o(t)$  is the predictor output, which is expected to reproduce the value that the input  $f$  would have  $\alpha$  seconds later, the mean-square error

$$\varepsilon = \lim_{T \rightarrow \infty} \frac{1}{2T} \int_{-T}^T \left[ f_o(t) - f(t + \alpha) \right]^2 dt \quad (22)$$

becomes, when eq. 20 is satisfied by the filter system function:

$$\varepsilon_{\min} = \frac{1}{2\pi} \int_0^{\alpha} \Psi^2(t) dt \quad (23)$$

Equations 17 through 23 are the fundamental predictor formulas.

## 2. Brief Historical Background

In an early paper, giving the first rigorous approach to the problem of "The Harmonic Analysis of Irregular Motion,"<sup>4</sup> N. Wiener credits G. I. Taylor for having introduced the concept of correlation in the study of irregular phenomena.<sup>2</sup> Autocorrelation functions for some simplified classes of time messages were computed by G. W. Kenrick,<sup>5</sup> as well as the corresponding power spectra or "frequency-energy distributions."

The fundamental mathematical tools for dealing with statistical functions extending through the infinite time range were developed by Wiener in his paper on "Generalized Harmonic Analysis."<sup>3</sup>

The general theory of filtering and prediction was given by the same author in 1942, as was previously mentioned.<sup>1,8</sup> The theory was made available by Y. W. Lee in a practical form, for direct use as a new technique of communication engineering.<sup>6</sup>

Use of the mean-square-error criterion in servomechanism design was attempted in a recent publication of the M.I.T. Radiation Laboratory Series.<sup>7</sup> However, the methods studied in the latter do not have the generality of Wiener's approach to the synthesis problem. Rather, the over-all structure of the servo system is given, and only the circuit coefficients are adjusted for optimum performance, in the presence of disturbances described by their autocorrelation function.

### 3. Purpose of the Present Paper

The wide range of possible practical applications of the new filter theory, suggested in the works of Wiener and Lee, have not been attempted as yet. A considerable amount of information has to be gathered before the various aspects of the theory can be applied to their full extent.

Before any significant practical achievement can be obtained, autocorrelation functions, or power spectra, must be computed from experimental records for various classes of signals.\* Several measurements are needed for each individual type of signal to establish the invariance of these statistical functions, since the theory applies to signals that are stationary time series, in "statistical equilibrium." In some cases, cross-correlation must be measured that may appear between interfering signals.

For these experimental data, suitable approximation criteria must be developed, ultimately leading to an analytical expression of the

---

\* An electronic autocorrelator is being built by T. Cheatham and E. Kretzmer at the M.I.T. Research Laboratory of Electronics.



system function that matches as closely as possible the theoretical performance.

In the present paper, an attempt is made to develop the techniques and outline limitations, in dealing with the pure predictor synthesis.

It is the author's belief that, besides its great possibilities of practical applications, the prediction problem is the most suitable for initial experimental work in connection with Wiener's theory. It is the simplest, since it deals with a single time function and requires computation of only one correlation function. The final result may be easily compared with the result expected from the theory. This verification of Wiener's theory by experiment, on the minimum mean-square-error basis, would be much more difficult for the filter problem, where more than one signal is involved. Besides, in the latter case, performance would also have to be compared with that of filters whose design follows the radically different criteria of the classical approach.

The prediction problem thus appears to afford a possible first insight into the mechanism of the new theory. Conclusions that may be derived from prediction studies will perhaps suggest analogous approaches, or prove to be directly applicable, to the general filter problem.

## CHAPTER II

### A Trial Experiment on Prediction

#### 1. Choice of the Input Function

For any random function, in statistical equilibrium, an optimum prediction operator may be derived by the methods of Wiener's theory, summarized in the last chapter.

Random functions are very common in nature: shot noise in electronic amplifiers, speech messages, pressure of wind gusts on the structure of airplanes in motion, turbulent flow of fluids, meteorologic records, etc.

A great number of these functions contain "hidden periodicities" arising, for example, from the alternation of seasons, or of day and night, in temperature records. In such cases it is evident that a very large number of experimental data, extending through a considerable range of time, is necessary for studying the true statistical character of the function; in other words, from an experimental point of view, a study of small records would not be adequate for verifying the condition of statistical equilibrium. In fact, temperature records extending through twelve hours of observations would give different statistical distributions according to whether the origin of time is taken at noon or at midnight, and according to the season, and perhaps to the cyclic variation of sun spots. For such functions the difficulty lies in the fact that they are generated by a great number of interfering factors. More likely to exhibit a stationary statistical character from small

records, are those functions which are produced by a limited number of known "agents" that can be isolated from other external conditions. Shot noise generated in a given amplifier belongs to this class of functions.

However, the above restrictions will become important in the constructive phases of applications of Wiener's methods, when filters will be required that operate steadily with a constant performance on a certain type of input functions. From the more academic point of view taken in this paper, where preliminary experimental examination is sought, the random function chosen for study needs to be stationary only in a local sense, within the range in which the experiment has to be performed.

The function chosen is shown in Fig. 1. It represents a latitudinal cross-section of the Rocky Mountains, extending across lands having a uniform geological pattern; the internal pressures of the earth that have given rise to the mountainous eruption, and the erosion that has taken place since, have therefore met with a reasonably uniform resistance of the ground surface within the range shown; a local stationary pattern may therefore be assumed along any section lying within the limits of the graph.

The problem is to compute a prediction operator for this function  $f(t)$ , for which arbitrary co-ordinates are chosen (Fig. 1), abscissae being interpreted in time rather than space units, in order to use the language and symbolism of Wiener's theory.

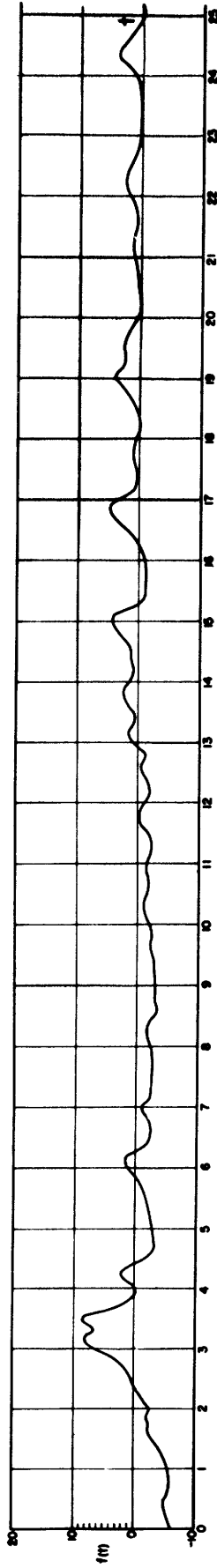


Figure 1.

## 2. Experimental Computation of Autocorrelation Function

Until some continuous autocorrelator is available,\* autocorrelation functions have to be approximated from finite experimental records. If the record extends from 0 to  $T_0$ , the approximate expression for eq. 17 is:

$$\varphi(\tau) = \frac{1}{T} \int_0^T f(t) f(t + \tau) dt, \quad T \leq T_0. \quad (24)$$

An integral has to be computed for each value of  $\tau$ .

Two procedures may be used, illustrated in Fig. 2 and 3.

In Fig. 2,  $T = T_0/2 = \text{constant}$ : The averaging process of eq. 24 is performed along a constant interval, for all values of  $\tau$  ranging from 0 to  $T_0/2$ . The same degree of accuracy is therefore obtained for the resulting  $\varphi(\tau)$ , when the variable  $\tau$  varies within these limits.

In Fig. 3, the averaging takes place over an interval  $T = T_0 - \tau$ , which decreases as the shifting parameter  $\tau$  increases. Equation 24 becomes:

$$\varphi(\tau) = \frac{1}{T_0 - \tau} \int_0^{T_0 - \tau} f(t) f(t + \tau) dt. \quad (25)$$

In this case the accuracy of  $\varphi(\tau)$  is greatly improved for small values of  $\tau$ , since the statistical data available from the record are used to a fuller extent. The accuracy decreases with increasing  $\tau$ , until it becomes equal to that obtained in the process of Fig. 2, when  $\tau = T_0/2$ .

In spite of its nonuniform accuracy, the process of Fig. 3 will be preferred, since the nature of the problem itself requires the greatest

---

\* See footnote, p. 8.

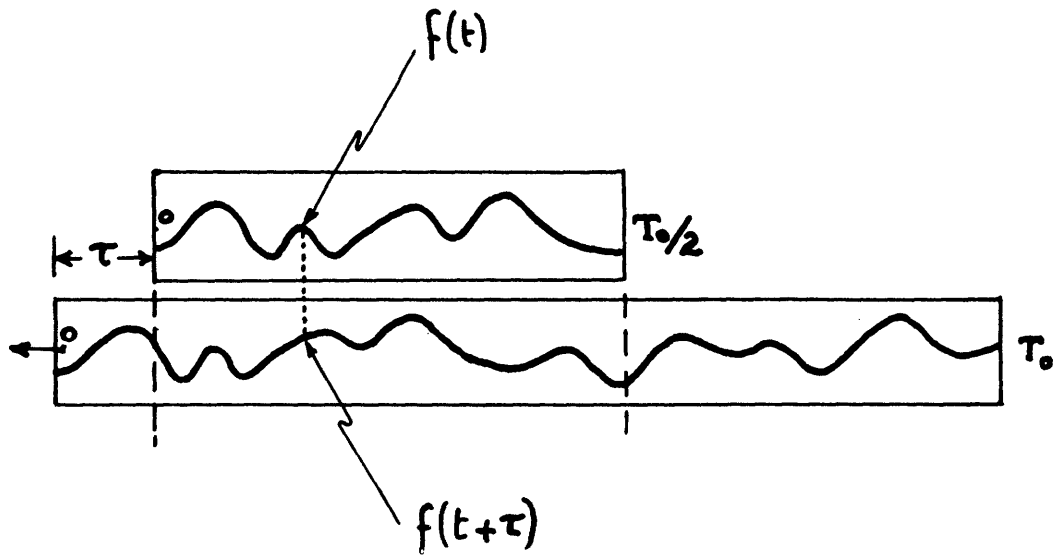


Fig. 2

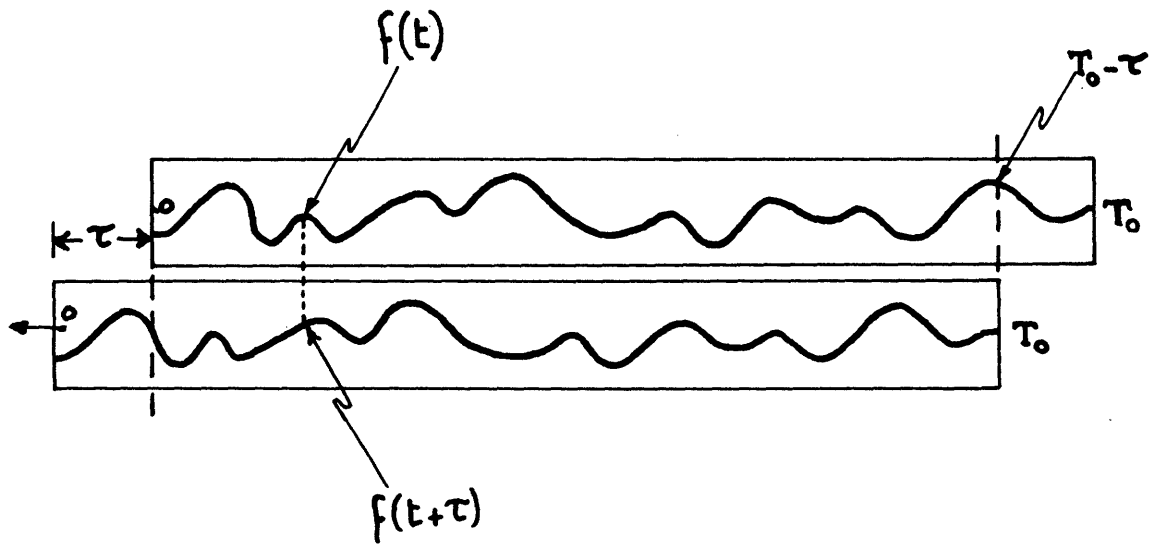
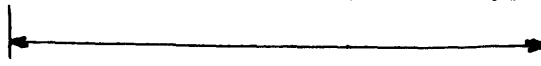


Fig. 3

possible precision for small values of shift  $\tau$ . Although this statement will be further elaborated in the following chapters, it is intuitive that the "correlation" described by  $\varphi(\tau)$ , between values of  $f(t)$  and values of  $f(t + \tau)$ , needs to be known very closely within the range of the functional "displacement" (lead or lag) that the filter must produce. In other words, if a lead or lag of  $\alpha$  seconds is required, the "dependence" between values of  $f(t)$  and values of  $f(t + \tau)$  taken by the function  $\tau$  seconds later, must be known with particular accuracy for  $\tau$  ranging between 0 and  $\alpha$ .

The autocorrelation function obtained from Fig. 1 is shown in Fig. 4, for  $\tau$  ranging between 0 and 5. The point-by-point computation was made for intervals  $\Delta\tau = 0.2$  between successive points. To that effect, ordinates of  $f(t)$ , read off Fig. 1, were listed for discrete values  $t = p \times 0.2$ , with  $p = 0, 1, 2 \dots 275$ . Let these ordinates be:  $f(0) = a$ ;  $f(0.2) = b$ ;  $f(0.4) = c$ ; ...  $f(55) = \ell$ . An identical list of values of  $f(t)$  was repeated along the former, "shifted" by an amount  $\tau = n \times 0.2$ . The resulting picture, shown below, is identical with the one described by Fig. 3. On the third line, products corresponding to values of the integrand of eq. 25 are computed.\*

<u>f(t)</u> :	a	b	c . . .	h	i	j	k	ℓ
<u>f(t + τ)</u> :	a	b	c	d	e . . .	j	k	ℓ
<u>f(t) f(t + τ)</u> :			ac	bd	ce . . .	hj	ik	jℓ
								
(276 - n) data (275 - n) intervals								

\*The tabulation shown corresponds to  $\tau = 0.4$ , or  $n = 2$ , but the argument is general.

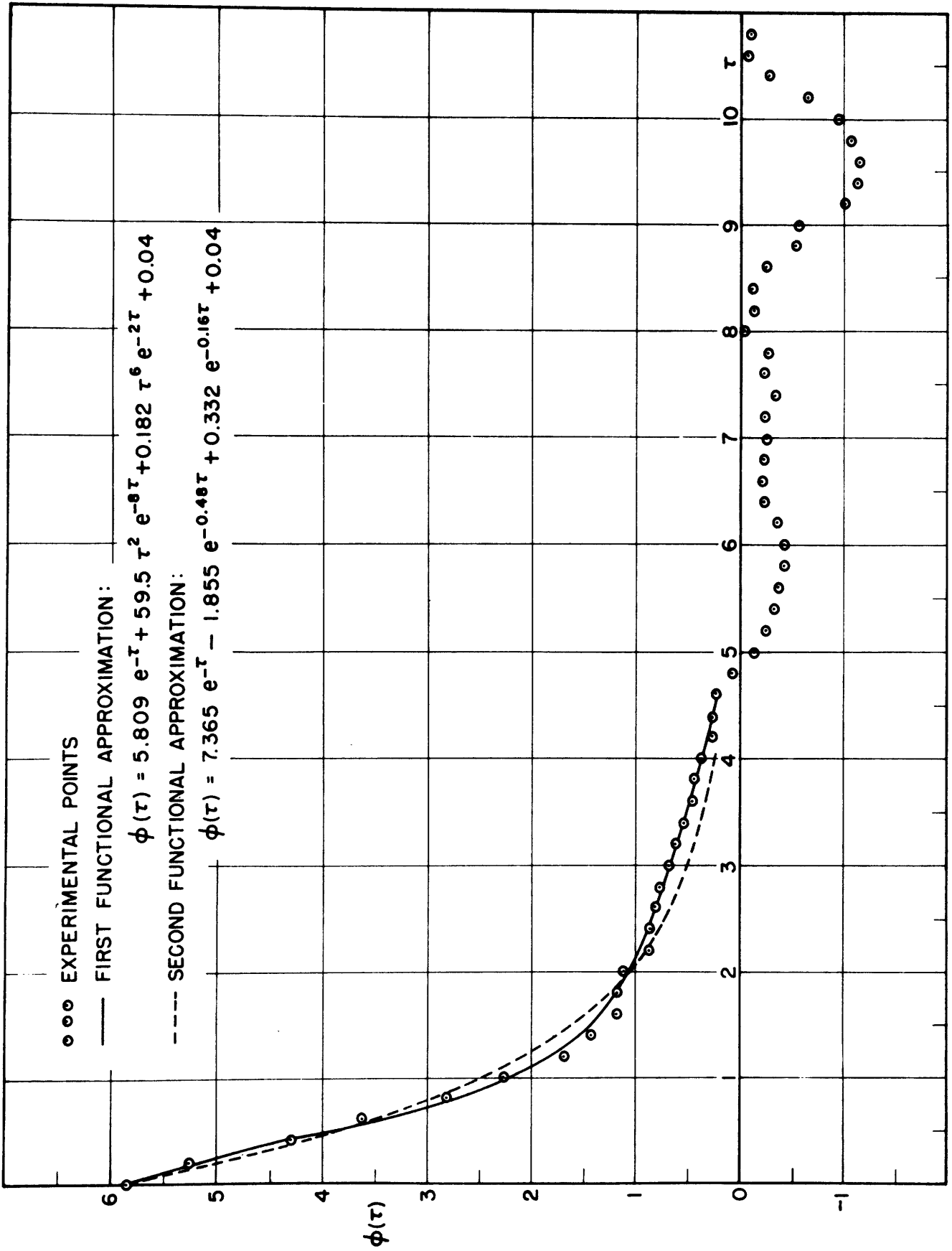


Fig. 4.



Values of the integrand  $f(t) f(t + \tau)$  are plotted in Fig. 5.

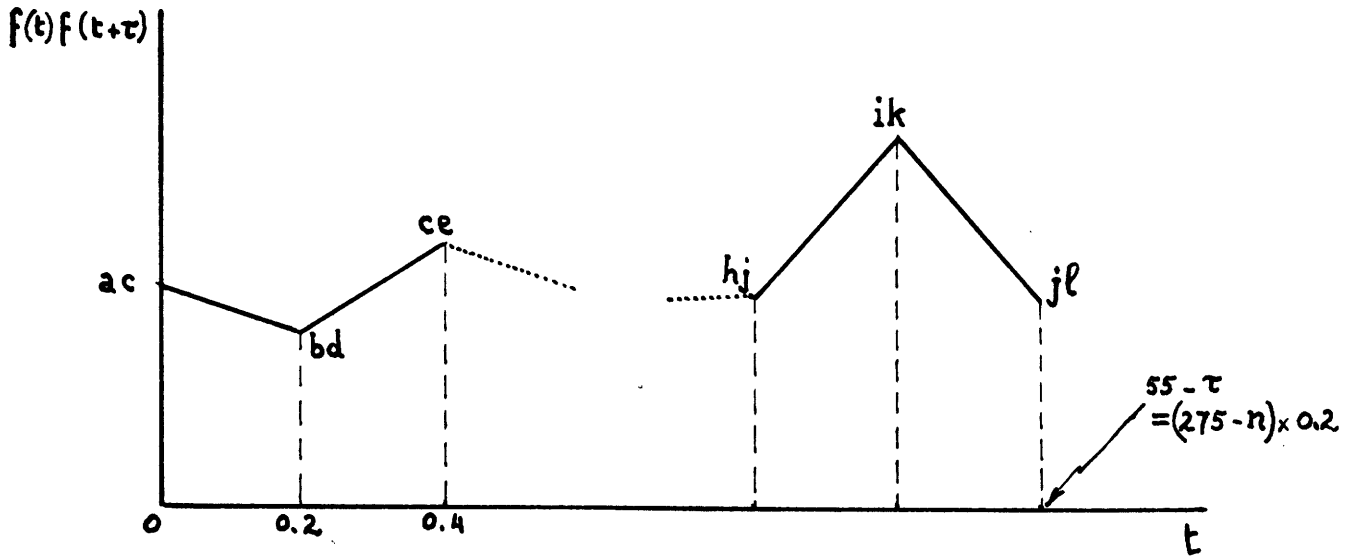


Fig. 5

The integral of eq. 25 is the area under the integrand curve of Fig. 5, for which the trapezoidal approximation shown gives:

$$\begin{aligned} \text{Area} &= 0.2 \times \left[ \frac{ac + bd}{2} + \frac{bd + ce}{2} + \dots + \frac{hj + ik}{2} + \frac{ik + jl}{2} \right] \\ &= 0.2 \times \left[ \frac{ac}{2} + bd + ce + \dots + hj + ik + \frac{jl}{2} \right] \\ &\approx \int_0^{T_0 - \tau} f(t) f(t + \tau) dt . \end{aligned}$$

The total interval, as shown on Fig. 5, is:

$$T_0 - \tau = (275 - n) \times 0.2 .$$

Equation 25 becomes:

$$\varphi(\tau) = \frac{1}{275 - n} \left[ \frac{ac}{2} + bd + ce + \dots + hj + ik + \frac{jl}{2} \right] , \quad (26)$$

with  $\tau = n \times 0.2$  .

Therefore  $\varphi(\tau)$  is obtained by summing all the column products of

the tabulation described above, the first and last products being halved, and dividing the resulting sum by  $275 - n$  .\*

### 3. Functional Approximation to Experimental Autocorrelation

The experimental points obtained in Fig. 4 show that the autocorrelation of  $f(t)$  goes very nearly to zero for increasing "shift"  $\tau$ . This is expected for a function that does not contain periodicities, provided its average value is zero. This statement will be considered rigorously correct, and local departures from this theoretical behavior will be considered as experimental errors arising from the finite range of the record.

In the case of Fig. 1, where the abscissa axis has been drawn arbitrarily, the average value of  $f(t)$  is not zero; its approximate expression yields:

$$f_{av} = \frac{\sum_{p=0}^{275} f(p \times 0.2)}{276} = -0.20 \quad , \quad (27)$$

where values of  $f(t)$  are taken, as before, at discrete intervals  $t = p \times 0.2$ , with  $p = 0, 1, 2 \dots 275$ .

Therefore it is the function

$$f_1(t) = f(t) - f_{av} \quad , \quad (28)$$

rather than  $f(t)$  itself, that has a zero average, and its corresponding autocorrelation

$$\varphi_1(\tau) = \lim_{T \rightarrow \infty} \frac{1}{2T} \int_{-T}^T f_1(t) f_1(t + \tau) dt \quad , \quad (29)$$

---

\*Calculations have been performed by the Computing Group of the M.I.T. Research Laboratory of Electronics.

rather than  $\varphi(\tau)$ , which must approach zero for increasing  $\tau$ .

We have:

$$\begin{aligned}\varphi_1(\tau) &= \lim_{T \rightarrow \infty} \frac{1}{2T} \int_{-T}^T [f(t) - f_{av}] [f(t + \tau) - f_{av}] dt, \\ \varphi_1(\tau) &= \lim_{T \rightarrow \infty} \frac{1}{2T} \int_{-T}^T f(t) f(t + \tau) dt + (f_{av})^2 \lim_{T \rightarrow \infty} \frac{1}{2T} \int_{-T}^T dt \\ &\quad - f_{av} \lim_{T \rightarrow \infty} \frac{1}{2T} \int_{-T}^T f(t) dt - f_{av} \lim_{T \rightarrow \infty} \frac{1}{2T} \int_{-T}^T f(t + \tau) dt.\end{aligned}$$

The last two integrals are equal, for a stationary time series, since they differ only in the choice of the origin of time; their common value is precisely  $f_{av}$ ; therefore,

$$\varphi_1(\tau) = \varphi(\tau) - (f_{av})^2. \quad (30)$$

For our case, from eq 27,  $(f_{av})^2 = 0.04$ , and it is the function

$$\varphi_1(\tau) = \varphi(\tau) - 0.04 \quad (31)$$

which must approach zero for increasing  $\tau$ .

The problem is to obtain an approximating function for  $\varphi_1(\tau)$  whose Fourier Transform  $\Phi(\omega)$  shall be rational in order to factorize it as  $\Phi(\omega) = \Phi^+(\omega) \Phi^-(\omega)$ , separating the singularities in the upper and lower half-planes.

Noticing that  $\varphi_1(\tau)$  is an even function of  $\tau$ , we get:

$$\Phi(\omega) = \frac{1}{2\pi} \int_{-\infty}^{\infty} \varphi_1(\tau) e^{-j\omega\tau} d\tau = \frac{1}{\pi} \int_0^{\infty} \varphi_1(\tau) \cos \omega\tau d\tau. \quad (32)$$

The condition that  $\Phi(\omega)$  be rational requires that  $\varphi_1(\tau)$  be expressed as a sum of exponentials of the forms

$$A e^{-a\tau} , \quad (33)$$

$$B \tau^n e^{-b\tau} , \quad (n \text{ integer}) \quad (34)$$

If  $\varphi_1(\tau)$  were oscillating about zero for small values of  $\tau$ , expressions of the form  $Ae^{-a\tau} \cos p\tau$  and  $B\tau^n e^{-b\tau} \cos q\tau$  could be used, leading to rational expressions for  $\Phi(\omega)$ . The condition that  $\varphi_1(\tau)$  approach zero for large values of  $\tau$  is met by using terms of the forms suggested above.

The method used for the approximation is now described. The experimental points of Fig. 4 are seen to follow the theoretical behavior for  $\tau$  ranging from 0 to 4.6; the approximation will be performed within this range.

Arbitrarily, we may choose to use a single term of the form  $Ae^{-a\tau}$ ; the corrective terms  $B\tau^n e^{-b\tau}$  that will be added will have a value zero for  $\tau = 0$ , and we are left with  $A = \text{actual ordinate of } \varphi_1(0) = 5.849 - 0.04 = 5.809$ . In order that the corrective terms be positive, we choose the value  $a = 1$ , which makes the exponential term  $Ae^{-a\tau}$  remain slightly below the  $\varphi_1(\tau)$  values for practically all the range considered. We now write:

$$\varphi_1(\tau) = 5.809 e^{-\tau} + \varphi_2(\tau) . \quad (35)$$

Values of  $\varphi_2(\tau)$  are computed in Appendix I and plotted in Fig. 6. They exhibit two maxima, around  $\tau = 0.25$  and  $\tau = 3$ , and need therefore be approximated by two terms of the form (34):

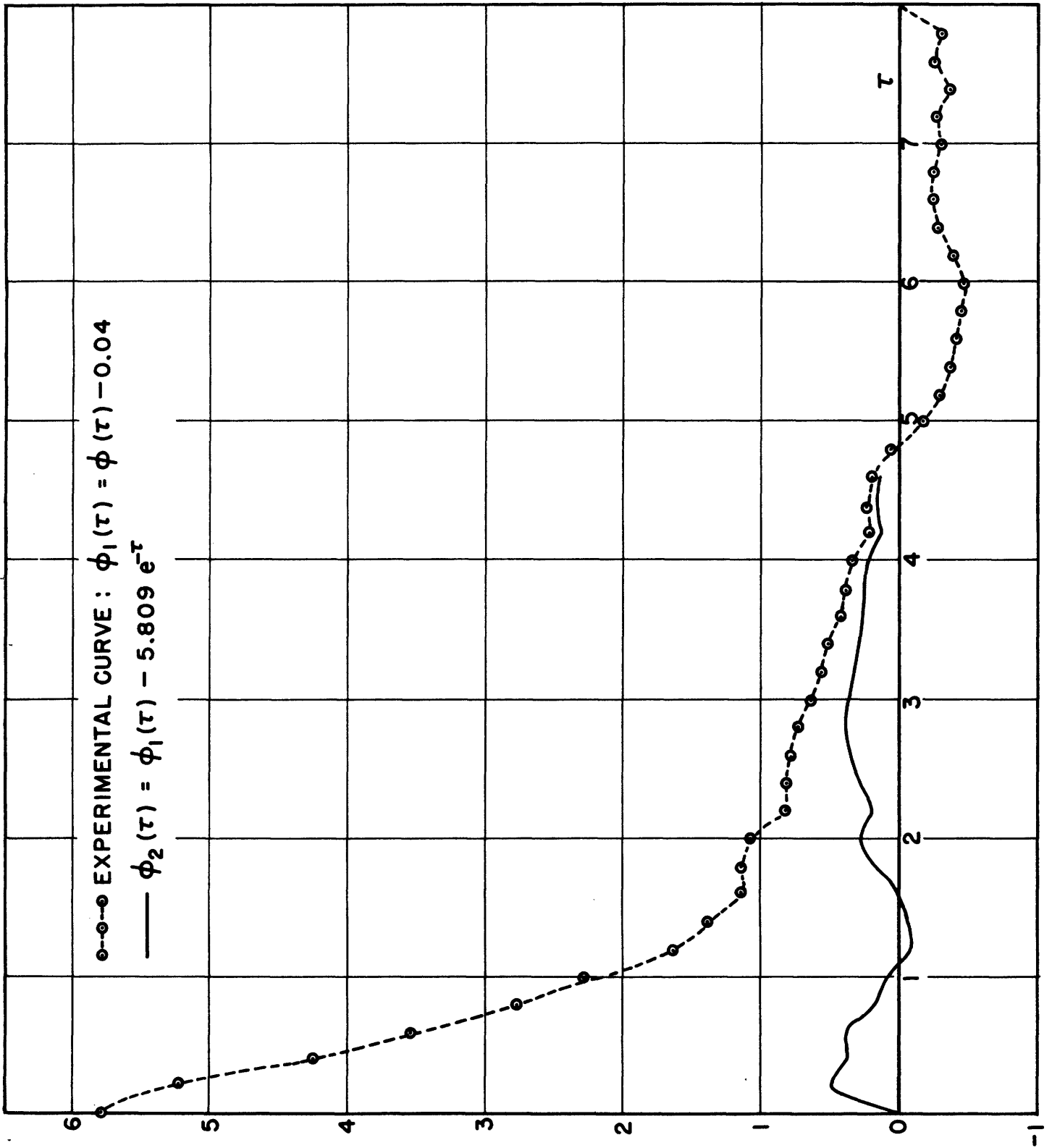


Figure 6

$$\varphi_2(\tau) = B\tau^n e^{-b\tau} + B'\tau^{n'} e^{-b'\tau}, \quad (36)$$

(n and n' integers).

Let us approximate the region of the first maximum with the term  $B\tau^n e^{-b\tau}$ . The maximum occurs for

$$B n \tau^{n-1} e^{-b\tau} - b B \tau^n e^{-b\tau} = 0, \quad (37)$$

$$\tau_M = \frac{n}{b}.$$

The corresponding maximum value of the term is

$$B \tau_M^n e^{-n}. \quad (38)$$

In our case,  $\tau_M = 0.25$ , and the corresponding value of  $\varphi_2$  is 0.5; this value will not be appreciably affected by the other additional term, whose maximum will occur at  $\tau = 3$ . We may write, therefore, according to (37) and (38):

$$n = 0.25 b, \quad (39)$$

$$B (0.25)^n e^{-n} = 0.5. \quad (40)$$

A third equation is needed, to solve for n, b, B; we may write that for  $\tau = 1$  (see Fig. 6) the value of the exponential must be very small; it must be appreciably smaller than the value (0.093) of  $\varphi_2(\tau)$ , since at  $\tau = 1$  the second corrective term will start being appreciable. Let, for example,

$$B (1)^n e^{-b(1)} = 0.02,$$

$$B e^{-b} = 0.02. \quad (41)$$

Using eq.39, eq.41 reads:

$$B e^{-4n} = 0.02. \quad (42)$$

Dividing (40) by (42), we get:

$$\begin{aligned} (0.25)^n e^{3n} &= 25 , \\ (0.25 \times e^3)^n &= 25 , \\ n &= 2 . \end{aligned} \quad (43)$$

Equations 39 and 41 give, respectively:

$$b = 8 , \quad B = 59.5 \quad (44)$$

Therefore eq.36 reads:

$$\varphi_2(\tau) = 59.5 \tau^2 e^{-8\tau} + B' \tau^{n'} e^{-b'\tau} . \quad (45)$$

Now the same procedure is applied to the second term, approximating the maximum of  $\varphi_2(\tau)$  occurring at  $\tau = 3$ ; since for  $\tau > 1$  the first term is negligible,  $\varphi_2(\tau)$  reduces to  $B' \tau^{n'} e^{-b'\tau}$  in this range, and the maximization gives:

$$n' = 3b' , \quad (46)$$

$$B' \times \left[ \frac{3}{e} \right]^{n'} = 0.35 , \quad (47)$$

A third equation is obtained by letting  $\varphi_2(\tau) = 0.25$  for  $\tau = 4$  (see Fig. 6):

$$B' \times 4^{n'} e^{-4b'} = 0.25 . \quad (48)$$

Again, solving (46), (47), and (48), we get:

$$B' = 0.182 , \quad n' = 6 , \quad b' = 2 \quad (49)$$

Replacing in eq.45,

$$\varphi_2(\tau) = 59.5 \tau^2 e^{-8\tau} + 0.182 \tau^6 e^{-2\tau} . \quad (50)$$

Finally, eq.35 reads:

$$\varphi_1(\tau) = 5.809 e^{-\tau} + 59.5 \tau^2 e^{-8\tau} + 0.182 \tau^6 e^{-2\tau} . \quad (51)$$

This function, plotted in Fig. 4 after addition of 0.04 to the ordinates (see eq. 31), is seen to give a very close approximation to the experimental data.\*

Expression 51 for  $\phi_1(\tau)$  could be used directly to compute the power spectrum, according to eq. 32. The process leads to an expression

$$\Phi(\omega) = \frac{P(\omega^2)}{Q(\omega^2)}$$

having a numerator of 10th degree and a denominator of 11th degree in  $\omega^2$ . The factorization of  $\Phi(\omega)$  requires therefore the solution of high-order equations if Expression 51 is used in its present form.

In order to simplify the problem, it is noticed that the high-order terms in  $\Phi(\omega)$  arise from the Fourier transformation (32) applied to terms of the form  $B\tau^n e^{-b\tau}$ . One must therefore try to approximate eq. 51 with terms of the form  $Ae^{-a\tau}$ , to the exclusion of other exponential forms. This leads to:

$$\phi_1(\tau) = \sum_p A_p e^{-a_p \tau}, \quad (52)$$

$$\Phi(\omega) = \frac{1}{\pi} \sum_p \int_0^\infty A_p e^{-a_p \tau} \cos \omega \tau d\tau,$$

$$\Phi(\omega) = \sum_p \frac{a_p A_p / \pi}{a_p^2 + \omega^2}. \quad (53)$$

If three terms are used in the expansion (52),  $\Phi(\omega)$ , when reduced to a common denominator, will have a numerator of 2nd degree in  $\omega^2$  and may be readily factorized.

---

\* Computations are tabulated in Appendix II.



The well-known procedure for obtaining the closest approximation to eq. 51 by an expansion of the form (52) is to use a set of normal-orthogonal function. Using the first three terms of the Legendre set, the optimum representation obtained for eq. 51 reads:\*

$$\varphi_1(\tau) = 7.365 e^{-0.8\tau} - 1.855 e^{-0.48\tau} + 0.332 e^{-0.16\tau}. \quad (54)$$

This function is plotted in Fig. 4.

Summarizing, the procedure leading to the workable approximation (54) consists of two steps: first, a function is sought that fits the experimental data with the least amount of cut-and-try techniques, and leads to Expression 51; next, an orthonormal expansion is computed for this function in order to obtain a more suitable expression (54) for further computational work.

#### 4. Optimum Predictor System Function

Expressions 52, 53, and 54 give directly:

$$\Phi(\omega) = \frac{1.877}{0.64 + \omega^2} - \frac{0.284}{0.23 + \omega^2} + \frac{0.0169}{0.0256 + \omega^2} = \frac{P(\omega)}{Q(\omega)} \quad (55)$$

After reduction to a common denominator, the numerator reads:

$$\begin{aligned} P(\omega) &= 1.61 \omega^4 + 0.3047 \omega^2 + 0.00884 \\ &= 1.61(\omega^2 + 0.1538)(\omega^2 + 0.0356) . \end{aligned}$$

Therefore,

$$\Phi(\omega) = \frac{1.61(\omega^2 + 0.1538)(\omega^2 + 0.0356)}{(0.64 + \omega^2)(0.23 + \omega^2)(0.0256 + \omega^2)} . \quad (56)$$

Separating the singularities lying in the upper and lower half planes,

---

\* Computations are performed in Appendix III.

we get, respectively:

$$\Phi^+(\omega) = \frac{1.27(0.392 + j\omega)(0.189 + j\omega)}{(0.80 + j\omega)(0.48 + j\omega)(0.16 + j\omega)}, \quad (57)$$

$$\Phi^-(\omega) = \frac{1.27(0.392 - j\omega)(0.189 - j\omega)}{(0.80 - j\omega)(0.48 - j\omega)(0.16 - j\omega)}. \quad (58)$$

Expanding eq. 57 in partial fractions yields:

$$\Phi^+(\omega) = \frac{1.543}{(0.80 + j\omega)} - \frac{0.317}{(0.48 + j\omega)} + \frac{0.0416}{(0.16 + j\omega)}. \quad (59)$$

Replacing this expression into eq. 21, we obtain directly:

$$\Psi(t + \alpha) = 2\pi \left[ 1.543 e^{-0.8(t+\alpha)} - 0.317 e^{-0.48(t+\alpha)} + 0.0416 e^{-0.16(t+\alpha)} \right]. \quad (60)$$

Replacing into eq. 20 yields:

$$H(\lambda) = \frac{1}{\Phi^+(\lambda)} \left[ \frac{1.543 e^{-0.8\alpha}}{(0.80 + j\lambda)} - \frac{0.317 e^{-0.48\alpha}}{(0.48 + j\lambda)} + \frac{0.0416 e^{-0.16\alpha}}{(0.16 + j\lambda)} \right].$$

Reducing to a common denominator and using for  $\Phi^+$  the expression found in eq. 57 yields:

$$H(\lambda) = \frac{L + M j \lambda + N(j \lambda)^2}{(0.392 + j \lambda)(0.189 + j \lambda)}, \quad (61)$$

with

$$L = 0.0933 e^{-0.8\alpha} - 0.032 e^{-0.48\alpha} + 0.0126 e^{-0.16\alpha},$$

$$M = 0.777 e^{-0.8\alpha} - 0.24 e^{-0.48\alpha} + 0.042 e^{-0.16\alpha},$$

$$N = 1.214 e^{-0.8\alpha} - 0.25 e^{-0.48\alpha} + 0.0328 e^{-0.16\alpha}.$$

For  $\alpha = 0$ , we get  $H(\lambda) = 1$ , which simply means that for zero prediction time, the system function, operating on the input  $f(t)$ , must be unity: If  $f(t)$  represented a voltage wave, the corresponding "filter" or "predictor" would be a simple open circuit.

### 5. Performance of the Prediction Operator

Let, for example,  $\alpha = 0.1$  . Replacing into (61) and expanding in partial fractions yields:

$$H(\lambda) = 0.9142 - \frac{0.00064}{0.392 + j\lambda} - \frac{0.0017}{0.189 + j\lambda} , \text{ for } \alpha = 0.1 .$$

It appears that the transfer function practically reduces to a constant 0.9142, the other terms being negligible. This means that, in the interval of time  $\alpha = 0.1$  , the function  $f(t)$  did not change very appreciably, and the optimum expression of this change is described by an over-all factor 0.9142 .

In order to make the frequency dependent terms of the system function more significant, we must choose a larger value of prediction time. However, we must remain within a range of time displacement where the function is highly correlated. From Fig. 4, a value  $\tau = 0.5$  of time displacement is seen to give still a reasonably large value of autocorrelation. We may therefore use  $\alpha = 0.5$  , for which eq. 61 becomes:

$$H(\lambda) = 0.6476 + \frac{0.01083}{0.189 + j\lambda} - \frac{0.0171}{0.392 + j\lambda} , \text{ for } \alpha = 0.5 . \quad (62)$$

This expression shows that, although we have chosen a prediction time sufficiently large (larger values would lead to poor performance, since they would exceed the range in which  $f(t)$  is well correlated), the prediction system function still reduces essentially to a constant. In fact, the frequency dependent terms, which become zero for large values of frequency  $\lambda$  , yield a maximum correction for zero frequency, of magnitude

$$\frac{0.01083}{0.189} - \frac{0.0171}{0.392} = 0.014 ,$$

which is still very small compared to the constant term 0.6476 .

This result is interpreted as follows: If we multiply all ordinates of the function

$$f_1(t) = f(t) - f_{av} = f(t) + 0.20^*$$

by the factor 0.6476, we obtain an "output" function\*\*

$$f_{01}(t) = f_0(t) + 0.20 = 0.6476 f_1(t) \quad (63)$$

which yields the closest possible approximation (in the mean-square-error sense) to the function  $f_1(t + 0.5)$ .

This result is clearly unsatisfactory; it may afford good prediction in regions of  $|f(t)|$  having small negative slope (see Fig. 1), since the predicting factor 0.6476 means that  $f(t)$  [actually  $f_1(t)$ ] should have decreased by that factor after an interval  $\alpha = 0.5$ ; but when the trend of  $|f(t)|$  is upward, prediction becomes very poor.

The actual experimental value of mean-square error, obtained by applying the prediction operator to the record of Fig. 1, is approximately<sup>+</sup>

$$\varepsilon = 2.95 . \quad (64)$$

From the definition of eq. 22, this means that the deviation, in absolute value, of the actual output  $f_0(t)$  from the output  $f(t + \alpha)$  expected

\* We recall that the axis of abscissae of  $f(t)$  had to be shifted in order to eliminate the average component of  $f(t)$ ; the prediction operator was derived for values  $f_1(t)$ , referred to the new axis. The predicted output  $f_{01}$ , therefore, also refers to the new axis, and corresponding readings  $f_0(t)$  for the original axis are given by eq 63.

\*\* For the more general case, in which  $H(\lambda)$  contains significant terms depending on  $\lambda$ , a computational method is described in Appendix IV, yielding numerical values of the output function from a given record of the input function.

<sup>+</sup> See Appendix V.

for perfect prediction, is in the average:  $\sqrt{\epsilon} = 1.72$  ; this error is considerably large, since inspection of Fig. 1 shows that values of  $f(t + \alpha)$  seldom exceed four to five units in magnitude. However, application of Wiener's theoretical expression for minimum error to the analytical developments of the preceding sections yields\*

$$\epsilon_{\min} = 3.15 \quad , \quad (65)$$

which is in good agreement with the experimental value (64).

These results suggest two alternative interpretations: Either the function of Fig. 1, whose behavior is described by its autocorrelation curve, does not lend itself to satisfactory prediction; or the accuracy of the functional approximation to the experimental values of correlation was not sufficient for deriving the actual optimum prediction operator.

Both interpretations focus attention upon the character of the autocorrelation curve. A systematic study of autocorrelation behavior is attempted in the following chapters, in order to derive: (a) criteria for the performance that may be expected from any given type of correlation curve, and (b) approximation requirements for an adequate use of experimental data.

---

\* See Appendix V.

## CHAPTER III

### Structural Relations Between Time Function and Autocorrelation Curve

#### 1. Fundamental Theorems

The signal function  $f(t)$  will be always considered to be of finite amplitude, of zero average, and in statistical equilibrium. The latter condition will be assumed to hold for all time derivatives of the function, designated by  $f'(t)$ ,  $f''(t)$  ...  $f^{(n)}(t)$ ; however, unless otherwise specified, these derivatives need not be finite.

It may be proved<sup>6</sup> that if

$$\varphi(\tau) = \lim_{T \rightarrow \infty} \frac{1}{2T} \int_{-T}^T f(t) f(t + \tau) dt, \quad (66)$$

then

$$\frac{d\varphi}{d\tau} = \varphi'(\tau) = \lim_{T \rightarrow \infty} \frac{1}{2T} \int_{-T}^T f(t) f'(t + \tau) dt, \quad (67)$$

and

$$-\frac{d^2\varphi}{d\tau^2} = -\varphi''(\tau) = \lim_{T \rightarrow \infty} \frac{1}{2T} \int_{-T}^T f'(t) f'(t + \tau) dt. \quad (68)$$

In other words:

Theorem I. The first derivative of the autocorrelation of the function equals the cross-correlation between the function and its time derivative. Symbolically, if

$$\varphi(\tau) = \varphi_{ff}(\tau), \quad (69)$$

then

$$\varphi'(\tau) = \varphi_{ff'}(\tau). \quad (70)$$

Theorem II. The negative of the second derivative of the auto-  
correlation of the function equals the autocorrelation of the time  
derivative of the function. Symbolically, if

$$\varphi(\tau) = \varphi_{ff}(\tau) , \quad (71)$$

then

$$- \varphi''(\tau) = \varphi_{f'f'}(\tau) . \quad (72)$$

Generalizing these properties for higher-order derivatives yields, with the type of notation used above:

$$(-1)^n \varphi^{(2n+1)}(\tau) = \varphi_{f^{(n)}f^{(n+1)}}(\tau) , \quad (73)$$

$$(-1)^n \varphi^{(2n)}(\tau) = \varphi_{f^{(n)}f^{(n)}}(\tau) , \quad (74)$$

where orders of derivatives are given by the superscripts (written in parentheses).

Referring to the expression defining the autocorrelation of a function  $f$ , it is seen that its value for  $\tau = 0$  is the mean value of  $f^2$ , written  $\overline{f^2}$ . From eq. 74, we have therefore:

$$\overline{[f^{(n)}]^2} = (-1)^n \varphi^{(2n)}(0) . \quad (75)$$

For example, for  $n = 1$  and  $n = 2$ :

$$\overline{f'^2} = - \varphi''(0) , \quad (76)$$

$$\overline{f''^2} = \varphi^{(4)}(0) . \quad (77)$$

Let us now return to eq. 67, which we repeat below:

$$\varphi'(\tau) = \lim_{T \rightarrow \infty} \frac{1}{2T} \int_{-T}^T f(t) f'(t + \tau) dt . \quad (67)$$

Integrating by parts gives:

$$\varphi'(\tau) = \lim_{T \rightarrow \infty} \frac{1}{2T} \left\{ f(t) f(t + \tau) \Big|_{-T}^T - \int_{-T}^T f(t + \tau) f'(t) dt \right\},$$

$$\varphi'(\tau) = \lim_{T \rightarrow \infty} \frac{1}{2T} \left[ f(T) f(T + \tau) - f(-T) f(-T + \tau) \right]$$

$$- \lim_{T \rightarrow \infty} \frac{1}{2T} \int_{-T+\tau}^{T+\tau} f(t) f'(t - \tau) dt .$$

The first term is zero, since the finite bracket is divided by the infinite quantity  $T$ . We are left with the second term, which may be written:\*

$$\varphi'(\tau) = - \lim_{T \rightarrow \infty} \frac{1}{2T} \int_{-T}^T f(t) f'(t - \tau) dt . \quad (78)$$

Comparing (67) and (78), we get:

$$\varphi'(\tau) = - \varphi'(-\tau) , \quad (79)$$

which states that  $\varphi'(\tau)$  is an odd function of  $\tau$ , a result which is apparent from the fact that  $\varphi(\tau)$  is an even function of  $\tau$ . But comparison of expressions (67) and (78) is particularly interesting when  $\tau$  approaches zero: If, for example,  $\tau$  goes to zero from the right in eq. 67, then  $(-\tau)$  goes to zero from the left in eq. 78; and, in the vicinity of zero, we may still write by eq. 79:

$$\varphi'(0+) = - \varphi'(0-) . \quad (80)$$

If both  $f(t)$  and  $f'(t)$  remain finite, the limiting process may be

---

\* Shifting the limits of integration is permissible, since  $f$  and  $f'$  are in statistical equilibrium.



carried to the very value  $\tau = 0$ , and yields:

$$\varphi'(0) = -\varphi'(0) = 0, \quad (81)$$

for  $f'(t)$  finite, which means that in this case the autocorrelation of  $f(t)$  has zero slope for  $\tau = 0$ . Repeating the same argument for  $f'(t)$ , it follows that its autocorrelation will also have zero slope at  $\tau = 0$ , provided  $f''(t)$  remains finite; recalling that the autocorrelation of  $f'(t)$  is also the negative second derivative of the autocorrelation of  $f(t)$ , we have:

Theorem III. If  $f(t)$ ,  $f'(t)$ , and  $f''(t)$  remain finite, both  $\varphi(\tau)$  and  $\varphi''(\tau)$  have zero slope at  $\tau = 0$ .

-----

Example (illustrating Theorem III)

Let  $f(t)$  be the function resulting from the algebraic sum of ordinates of overlapping pulses of the form  $A(t) = t^2 e^{-t}$ , starting on the time axis and occurring at random at the average rate of  $k$  pulses per second, with equal probability of being positive or negative (Fig. 7a). The individual pulses are seen to have no steep rises and no sharp corners. Their first and second derivatives remain therefore finite, and the same applies to the resulting function  $f(t)$ .

The autocorrelation of the resulting function may be shown<sup>6</sup> to reduce to the expression:

$$\varphi(\tau) = k \int_0^{\infty} A(t) A(t + \tau) dt = \frac{k}{4} e^{-|\tau|} \left[ \tau^2 + 3|\tau| + 3 \right], \quad (82)$$

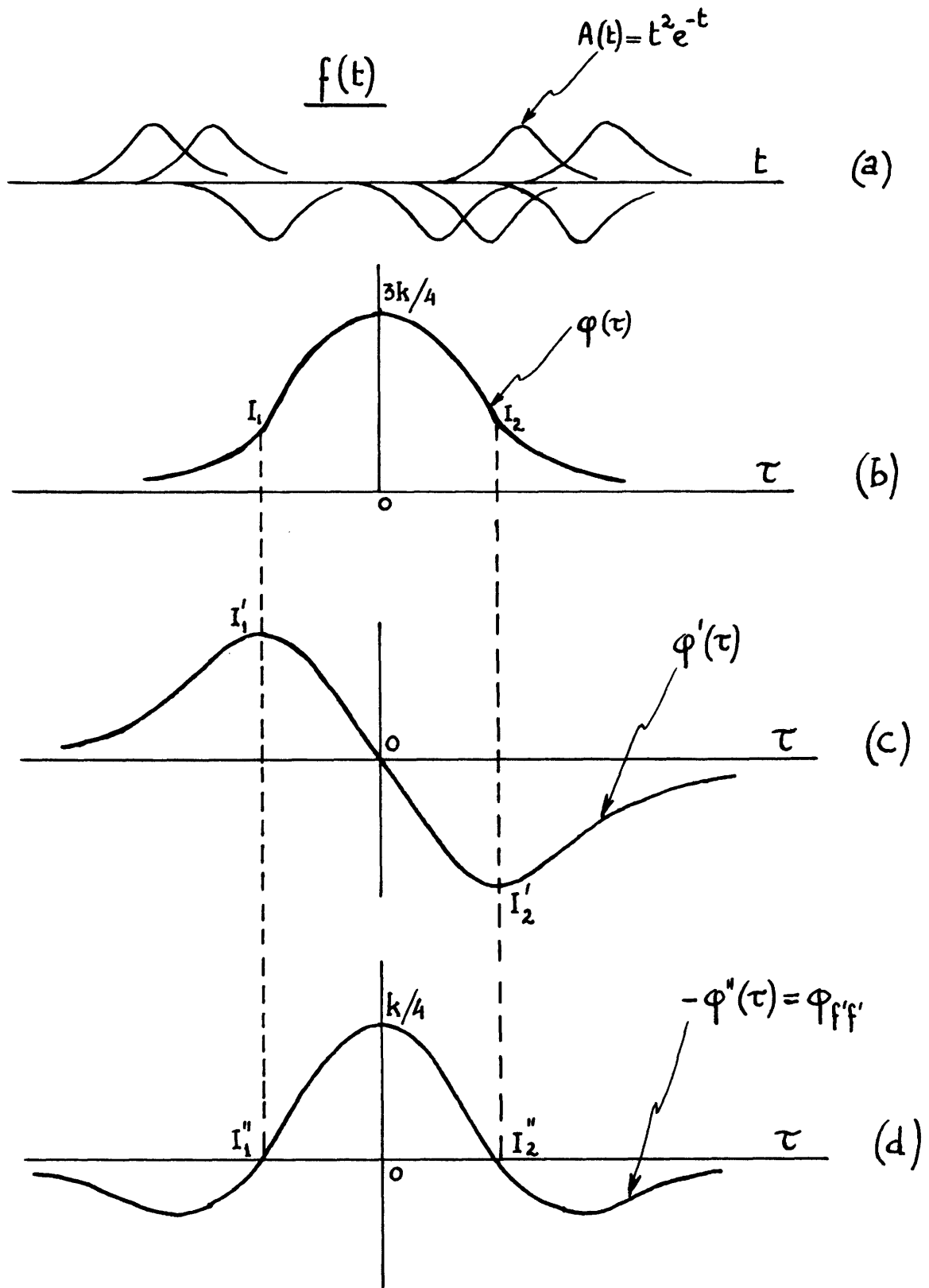


Figure 7

Correlation functions for finite  $f$ ,  $f'$  and  $f''$  (Theorem III).

yielding:

$$\varphi'(0) = 0, \quad (83)$$

$$-\varphi''(0) = \frac{k}{4} \quad \left[ = \varphi_{f,f'}(0) \right] \quad (84)$$

$$-\varphi'''(0) = 0 \quad \left[ = \varphi_{f',f'}'(0) \right]. \quad (85)$$

These results are in agreement with Theorem III, eqs 83 and 85 representing, respectively, the slopes of  $\varphi(\tau)$  and  $\varphi''(\tau)$  for  $\tau = 0$ . Equation 84, compared with eq. 76, gives the average square derivative of the function, a positive finite quantity as expected. Figure 7 illustrates these results.

-----

If the second derivative of the function is not finite, the argument leading to Theorem III does not hold for  $\varphi''(\tau)$ .

Theorem IV. If only  $f(t)$  and  $f'(t)$  remain finite,  $f''(t)$  becoming infinite,  $\varphi(\tau)$  has zero slope for  $\tau = 0$ , but  $\varphi''(\tau)$  does not.

-----

Example (illustrating Theorem IV)

The function  $f(t)$  will be defined as in the preceding example, the individual pulses being this time of the form  $A(t) = t e^{-t}$ , as shown in Fig. 8a. The first derivative remains finite, since there are no steep rises; but the second derivative becomes infinite, since individual pulses start from the time axis with a sharp corner (infinite rate of change of first derivative). We have:

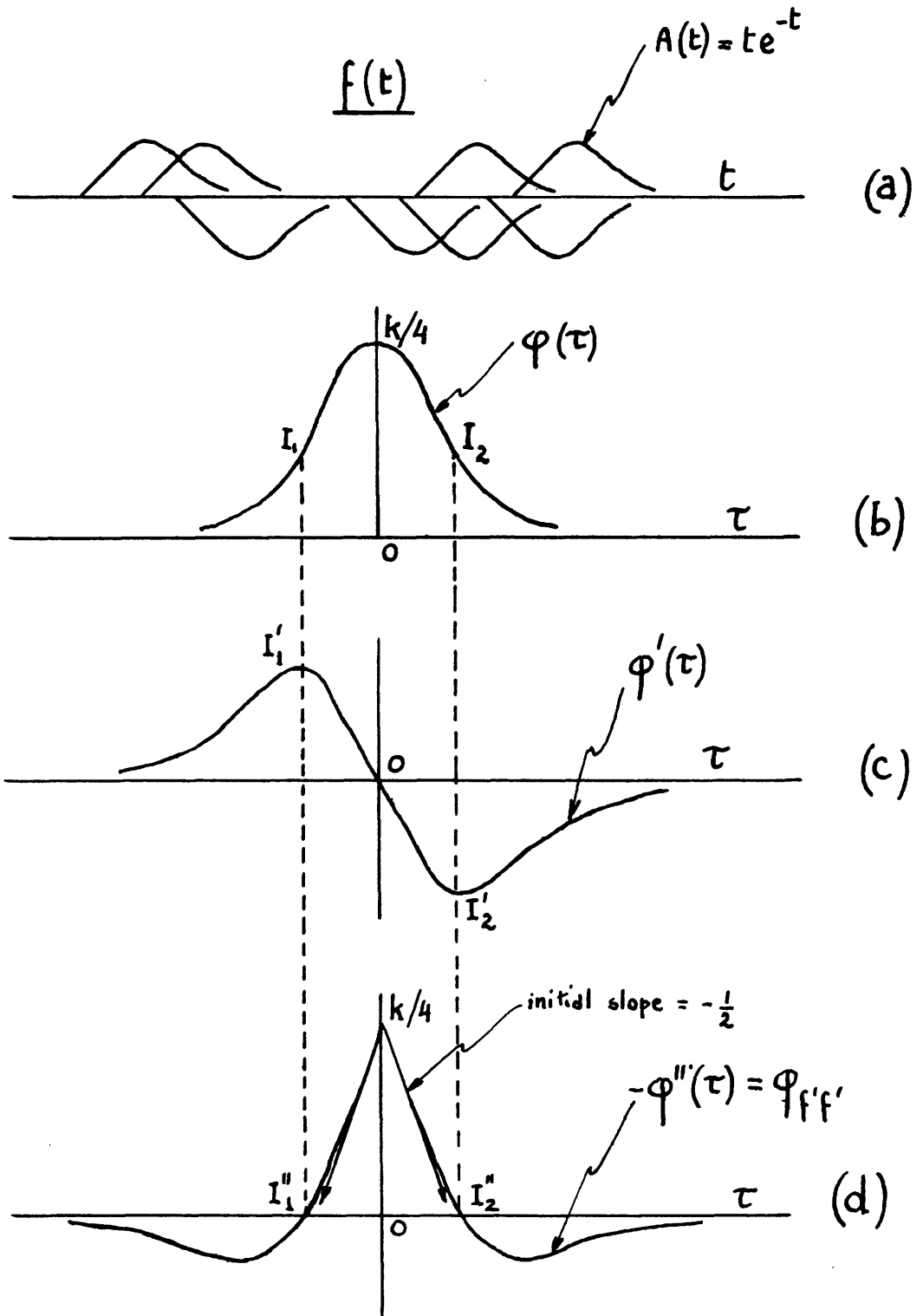


Figure 8

Correlation functions for finite  $f$  and  $f'$ , infinite  $f''$  (Theorem IV).

$$\varphi(\tau) = k \int_0^{\infty} A(t) A(t + \tau) dt = \frac{k}{4} e^{-|\tau|} \left[ |\tau| + 1 \right], \quad (86)$$

yielding:

$$\varphi'(0) = 0, \quad (87)$$

$$-\varphi''(0) = \frac{k}{4} \left[ = \varphi'_{f'f'}(0) \right], \quad (88)$$

and

$$-\varphi''(0+) = -\frac{1}{2} \left[ = \varphi'_{f'f'}(0+) \right]. \quad (89)$$

Figure 8 illustrates these results, which are in agreement with Theorem IV.

-----

The result of eq. 89, which agrees with the statement of Theorem IV, may be given another interpretation; actually, according to Theorem II, it represents the slope of the autocorrelation  $\varphi_{f'f'}$  of the derivative function  $f'(t)$ . It is seen that this slope is not zero when the derivative  $f''(t)$  of the function  $f'(t)$  is not finite. Applying this property to  $f(t)$  and  $f'(t)$  instead of  $f'(t)$  and  $f''(t)$ , gives the following theorem:

Theorem V. If  $f(t)$  has a derivative  $f'(t)$  which becomes infinite, the autocorrelation  $\varphi(\tau)$  does not have zero slope at the point  $\tau = 0$ , but has symmetrical slopes about this point. Therefore, point  $\tau = 0$  is in this case an angular point for the curve  $\varphi(\tau)$ .

It is therefore recognized that the limiting process leading to eq. 81 cannot be carried to the very value  $\tau = 0$ , but only to values at the right and at the left of zero, as expressed by eq. 80. According to Theorem V, the latter equation must be rewritten as follows:

$$\varphi'(0+) = -\varphi'(0-) \neq 0 \quad (90)$$

if  $f'(t)$  becomes infinite.

Theorem V is already illustrated by Fig. 8d, where the function  $f(t)$  is replaced by  $f'(t)$ . A direct example is given below.

-----

Example (illustrating Theorem V)

The function  $f(t)$  will be defined as in the previous examples, the individual pulses being this time of the form  $A(t) = e^{-t}$ , as shown in Fig. 9a. The resulting function remains finite, but it is seen to have sharp rises which make its derivative become infinite.

We have:

$$\varphi(\tau) = k \int_0^{\infty} A(t) A(t + \tau) dt = \frac{k}{2} e^{-|\tau|}, \quad (91)$$

which is drawn in Fig. 9b and illustrates Theorem V and eq. 90; also, according to the latter, values at  $0+$  and  $0-$  of the function  $\varphi'(\tau)$  appearing in Fig. 9c are seen to be opposite:

$$\varphi'(\tau) = -(\text{sign of } \tau) \frac{k}{2} e^{-|\tau|}. \quad (92)$$

The function  $-\varphi''(\tau)$  is shown in Fig. 9d:

$$-\varphi''(\tau) = -\frac{k}{2} e^{-|\tau|}. \quad (93)$$

It must be understood that the plots of Fig. 9c and 9d have significance only for  $\tau > 0$  and  $\tau < 0$ , but not for the very value  $\tau = 0$ . Actually, if we assign the value  $-\frac{k}{2}$  to  $-\varphi''(0)$ , as would appear from Fig. 9d, we must conclude from eq. 76 that the average value of  $f'^2$  is a negative number, which is obviously incorrect. As a matter of fact, we know in this case that  $\overline{f'^2} = \infty$ . Also, from Theorem II, Fig. 9d is the autocorrelation of the derivative function  $f'(t)$ . It would be incorrect to say that this derivative function is obtained by

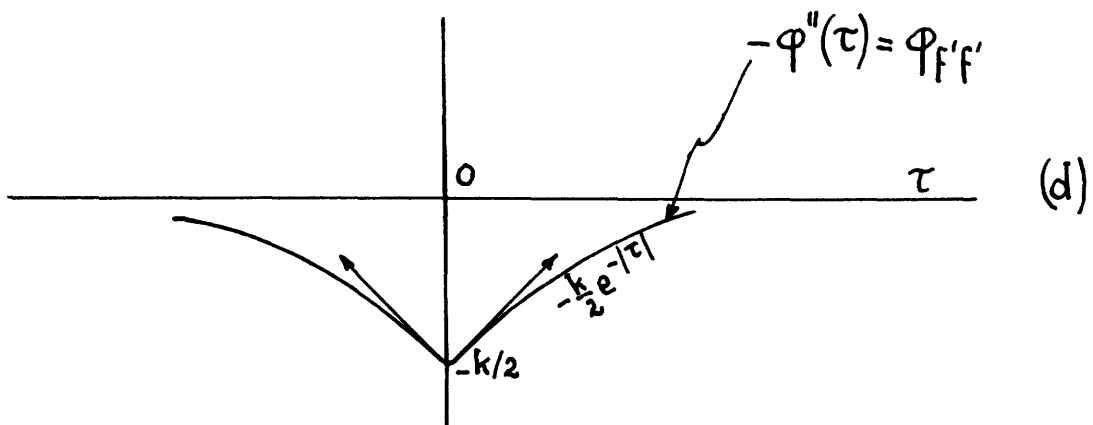
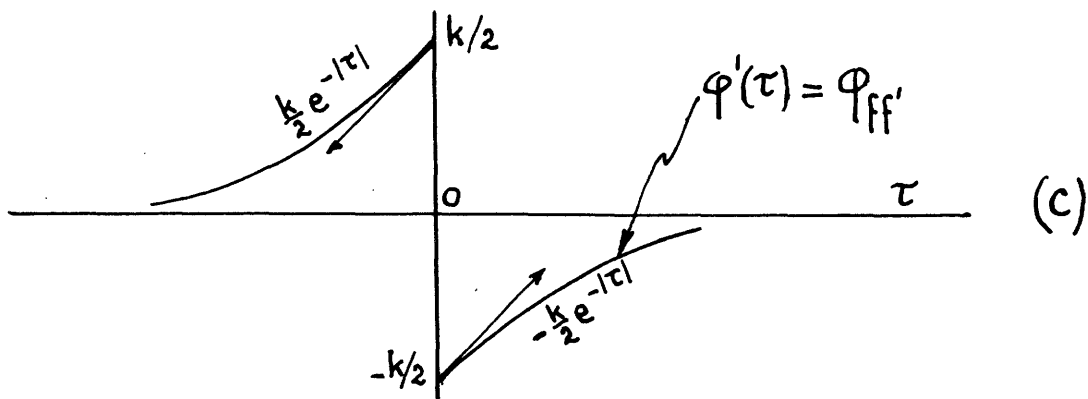
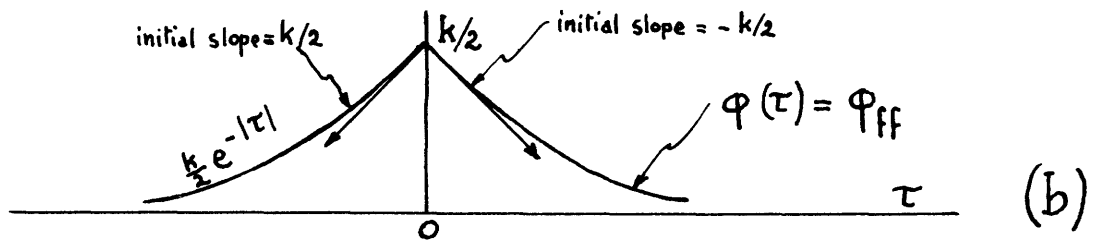
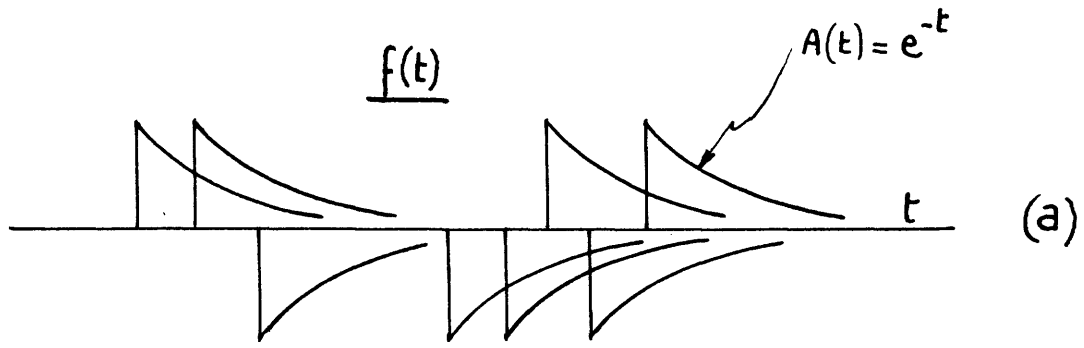


Figure 9

a superposition of derivative pulses of the form  $-e^{-t}$ ; actually, the correct derivative pulses start with an infinite impulse, after which they become of the form  $-e^{-t}$ .

Explanation of Fig. 9d is illustrated by Fig. 10 and the following heuristic argument.

Figure 10a shows two typical pulses of the  $f(t)$  function (from Fig. 9a). Figure 10b shows the corresponding derivative curve. Infinite derivative at a point is interpreted as an impulse in the derivative curve, with area equal -- in magnitude and sign -- to the corresponding "jump" of the time function  $f(t)$ . This description verifies the requirement that  $f(t)$  must be the integral of its derivative curve.

Now the autocorrelation  $\phi_{f',f'}$  of the derivative curve must be evaluated, and justify the form of Fig. 9d. Applying a property already used in the text, we call  $A'(t)$  a single derivative pulse consisting (as shown in Fig. 10c) of a unit impulse followed by  $-e^{-t}$ . For the average rate of  $k$  pulses per second, the autocorrelation of the resulting function  $f'(t)$  is given by

$$\phi_{f',f'}(\tau) = k \int_0^{\infty} A'(t) A'(t + \tau) dt . \quad (94)$$

It will be convenient to separate in this integral the contributions of the impulse and the exponential  $-e^{-t}$ . The impulse will be considered as the limit, for  $\Delta t \rightarrow 0$ , of a rectangle of width  $\Delta t$  and height  $\frac{1}{\Delta t}$  (area = 1, for the function considered).

For  $\tau = 0$ , the contribution of the impulse to integral (94) is:

$$\lim_{\Delta t \rightarrow 0} \int_0^{\Delta t} \left[ \frac{1}{\Delta t} \right]^2 dt = \lim_{\Delta t \rightarrow 0} \left[ \frac{1}{\Delta t} \right]^2 \Delta t = \infty ; \quad (95)$$



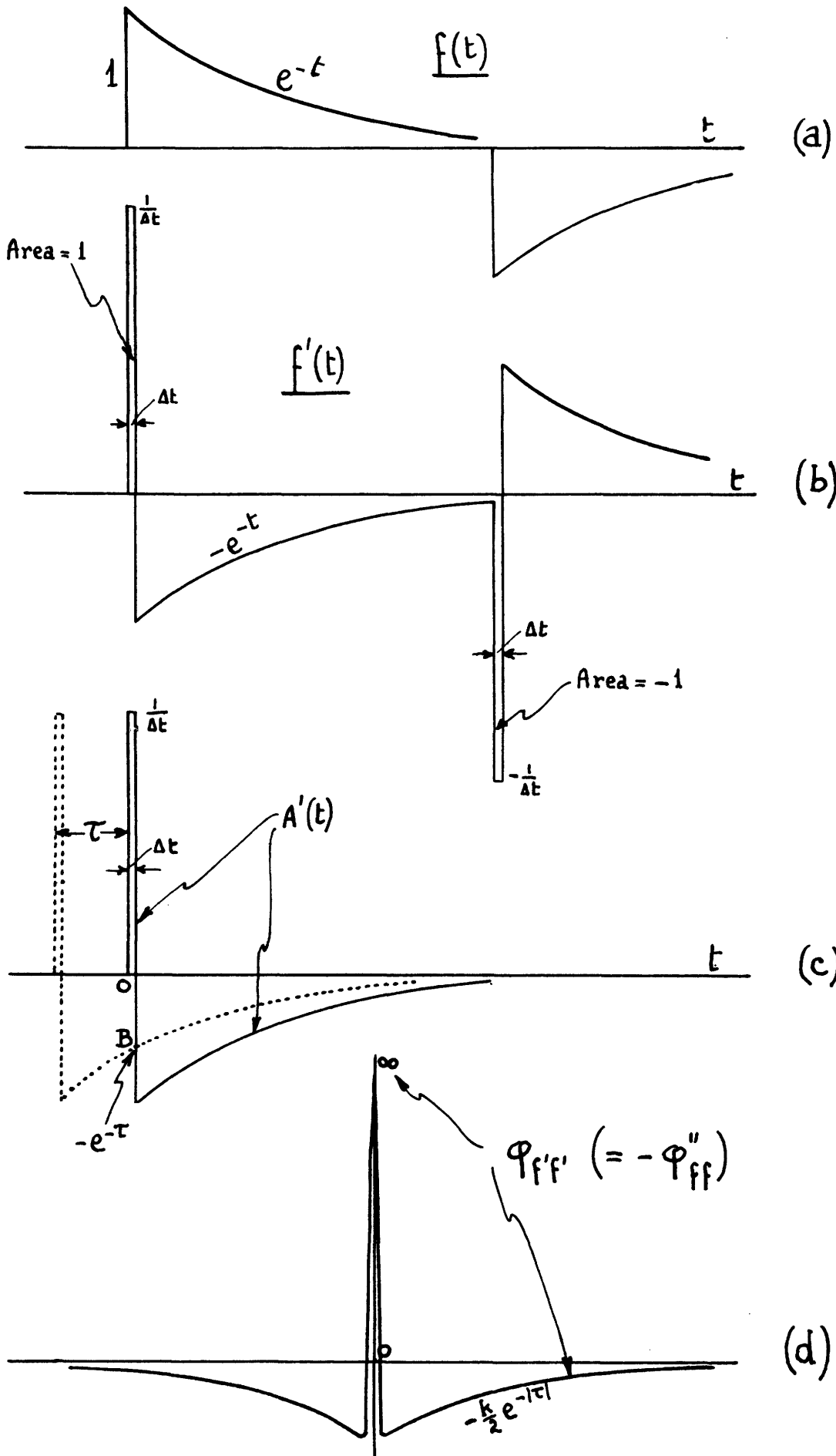


Figure 10

the contribution of the exponential being finite, we have the result:

$$\varphi_{f'f'}(0) = \omega \quad (96)$$

Under a finite displacement  $\tau$ , the impulses, of differential width, do not overlap (Fig. 10c), even for very small  $\tau$  (for example, for  $\tau = 0^+$ ). The contribution of the impulse to the integral (94) is

$$\lim_{\Delta t \rightarrow 0} k \int_0^{\Delta t} \frac{1}{\Delta t} \left[ -e^{-\tau} \right] dt = \lim_{\Delta t \rightarrow 0} -\frac{k}{\Delta t} e^{-\tau} \int_0^{\Delta t} dt = -ke^{-|\tau|},^* \quad (97)$$

and the contribution of the exponential is

$$k \int_0^{\infty} \left[ -e^{-t} \right] \left[ -e^{-(t+\tau)} \right] dt = \frac{k}{2} e^{-|\tau|}, \quad (98)$$

identical with (91). Equation 98 would be the positive autocorrelation expected for the derivative pulse if we neglected the initial infinite portion. Adding the contributions (97) and (98) to integral (94), we obtain:

$$\varphi_{f'f'}(\tau) = -\frac{k}{2} e^{-|\tau|} \quad \text{for } \tau \neq 0. \quad (99)$$

Results (96) and (99) are illustrated in Fig. 10d, which in the limit becomes identical with Fig. 9d and explains the behavior of  $\varphi_{f'f'}$  at  $\tau = 0$ . Figure 10d appears as a limiting case of Fig. 8d, where points  $I_1''$  and  $I_2''$  are compressed against the ordinate axis.\*\*

\* Notice that this contribution is equal to  $k$  times the ordinate OB of the displaced curve, at the level of the impulse (Fig. 10c).

\*\* As well as the corresponding inflection points  $I_1$  and  $I_2$  of Fig. 8b are compressed against the ordinate axis in Fig. 9b.

-----

Inspection of Fig. 10 allows us to draw a general proof of Theorems IV and V. We first recall that the radius of curvature of a function  $\varphi$  is given by the expression

$$R = \frac{[1 + \varphi'^2]^{3/2}}{\varphi''} . \quad (100)$$

The sign of  $R$  is the same as the sign of  $\varphi''$ , and has the following interpretation:

(a) If  $R > 0$  (or  $\varphi'' > 0$ ), the circle of curvature lies above the  $\varphi$ -curve, which is said to have "positive curvature" (Fig. 11a).

(b) If  $R < 0$  (or  $\varphi'' < 0$ ), the circle of curvature lies below the  $\varphi$ -curve, which is said to have "negative curvature" (Fig. 11b).

(c) If  $R = 0$  (or  $|\varphi''| = \infty$ ), the circle of curvature reduces to a point, and the  $\varphi$ -curve has "infinite curvature"\* at this point, which becomes an angular point (Fig. 11c and 11d).

We read from Fig. 11a that whenever the function  $\varphi$ , interpreted as the autocorrelation of  $f(t)$ , has positive curvature, the autocorrelation of  $f'(t)$  is negative (compare Fig. 9b and 9d). Figure 11d indicates that when  $-\varphi'' = \infty$ , then  $\varphi$  has an angular point (compare Fig. 9b and 10d); this occurs precisely when  $f'(t)$  assumes infinite values, since in that case  $\overline{f'^2} = \infty$ , giving  $-\varphi''(0) = \infty$  (see eq 76).

Let us now investigate the types of pulses  $A(t)$  that will give negative curvature for  $\varphi$  at  $\tau = 0+$  and  $\tau = 0-$ , when  $\varphi(0)$  is an

---

\* Expressions "infinite curvature" and "zero radius of curvature" are therefore equivalent. The first one pictures the sharpness of the turn made by the curve; the second refers to the small circle around which the turn is made.

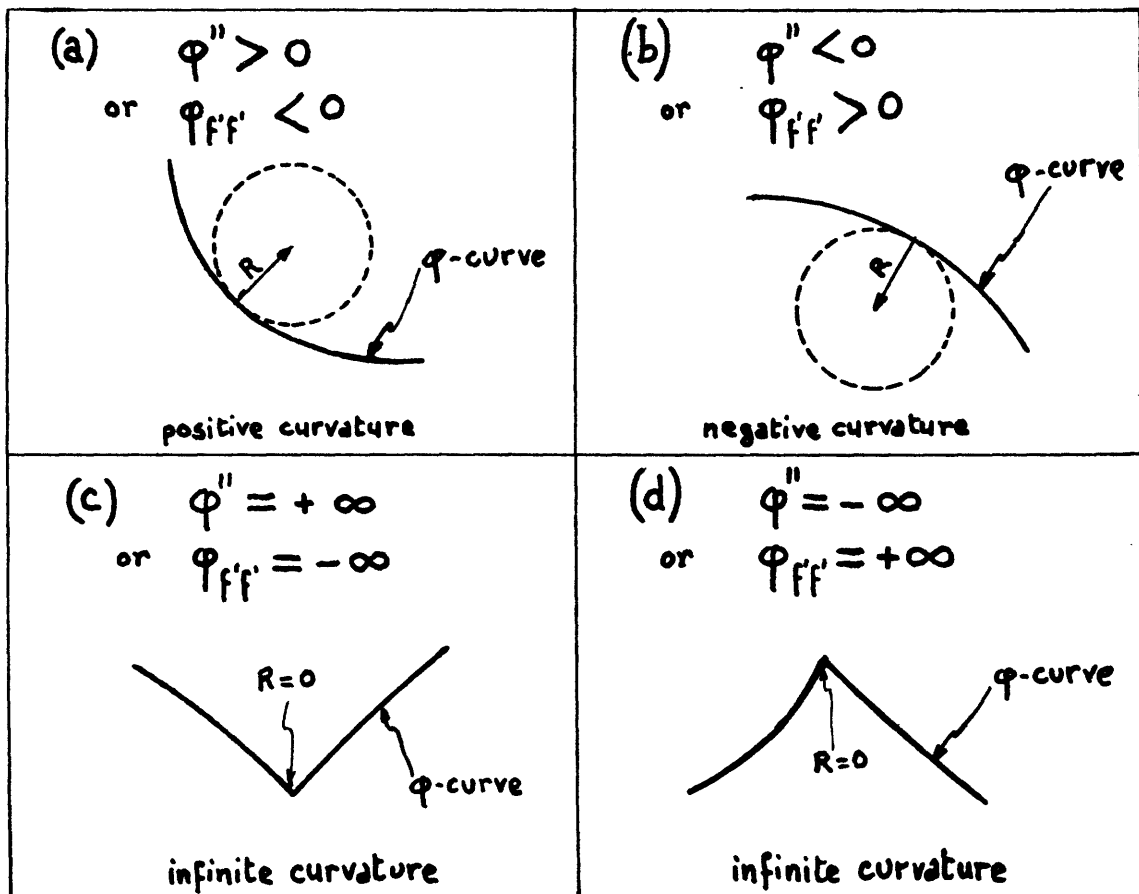


Fig. 11

angular point ( $A'(t)$  becoming infinite). The analysis of Fig. 10 has shown that for pulses of the type  $e^{-t}$ , the curvature of  $\varphi$  is positive ( $\varphi_{f'f'}$ , negative), as shown in Fig. 9b. This resulted from the fact that the negative contribution (97) of the derivative impulse to integral (94) was larger than the positive contribution (98) of the area of the finite derivatives squared. If we can reduce the negative contribution of the impulse to zero, or even make it positive, then  $\varphi_{f'f'}$  will certainly be positive for  $\tau = 0+$  or  $0-$ , and  $\varphi(\tau)$  will have a negative curvature near zero. Recalling that the contribution of the impulse reduces to the ordinate  $OB^*$  of the derivative pulse for

\* See footnote, p. 42.

an abscissa  $\tau$ , we see that the requirement is met if the derivative is zero or positive after the vertical rise. This leads to the following theorem for the resulting function  $f(t)$ :

Theorem VI. If  $f(t)$  contains vertical rises ( $f'(t)$  infinite), immediately followed by a slope which is positive or zero (nonconstant) in the average, the autocorrelation  $\varphi(\tau)$  has negative curvature in the vicinity of  $\tau = 0$ . The point  $\tau = 0$  is still an angular point.\*

-----

Example (illustrating Theorem VI)

The function  $f(t)$  is defined as in previous examples, the individual pulses being now of the form  $A(t) = (1 + t)e^{-t}$ , shown in Fig. 12a. The sharp rises of the pulses are followed by horizontal slopes, and the resulting function  $f(t)$  meets the conditions of Theorem VI, of having jumps followed by a zero, nonconstant slope in the average. We have:

$$\varphi(\tau) = \frac{k}{4} e^{-|\tau|} (3|\tau| + 5) \quad (101)$$

and

$$-\varphi''(\tau) = \frac{k}{4} e^{-|\tau|} (1 - 3|\tau|). \quad (102)$$

Function (102) is shown in Fig. 12c, where the point at infinity, arising from analysis of Fig. 12b, is also included. The positive values of  $-\varphi''$  for  $\tau = 0+$  and  $0-$  yield, as expected, a negative curvature for  $\varphi(\tau)$  around  $\tau = 0$  (Fig. 12d).

---

\* From Theorem V, since  $f'(t)$  becomes infinite.

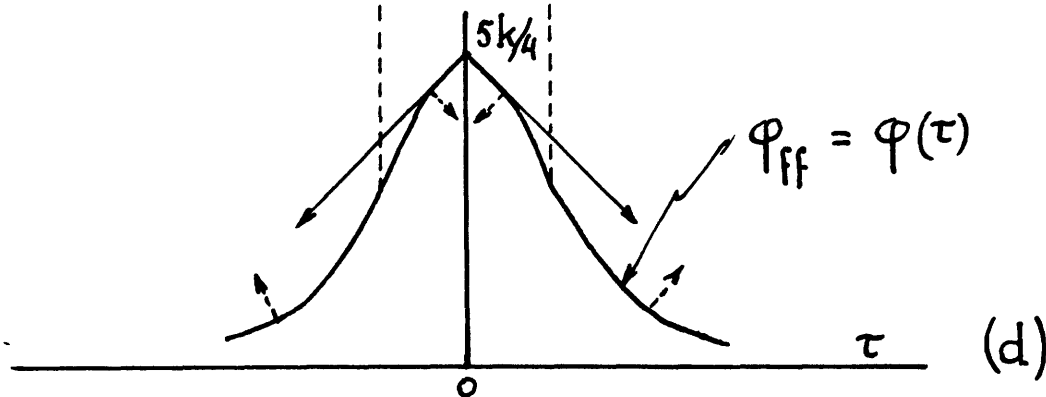
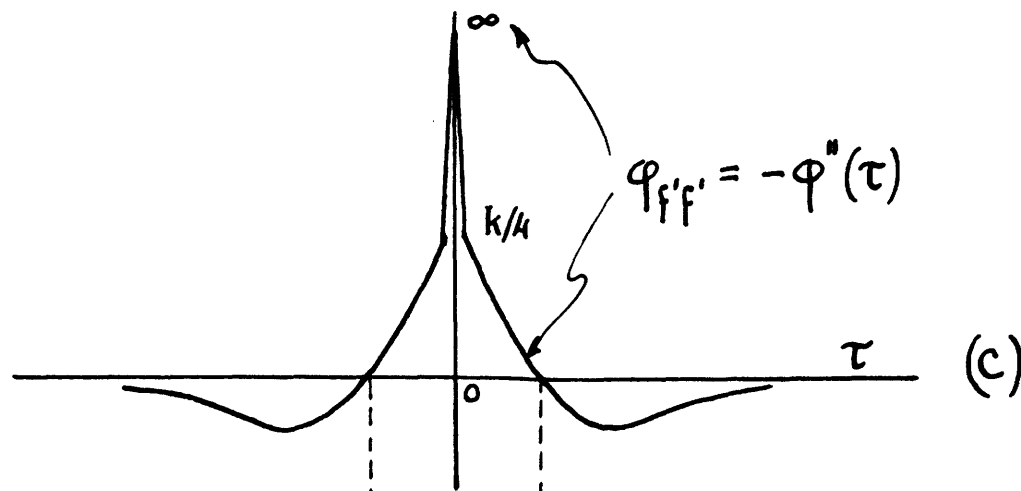
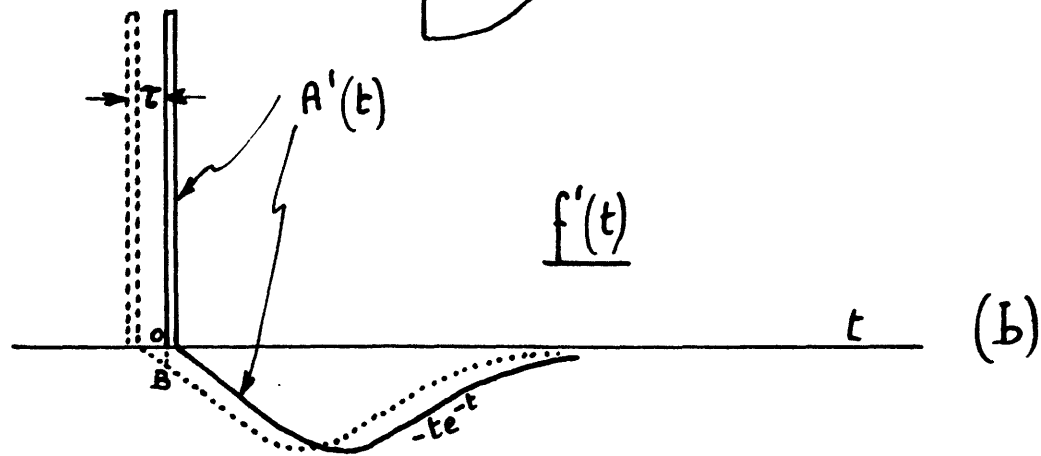
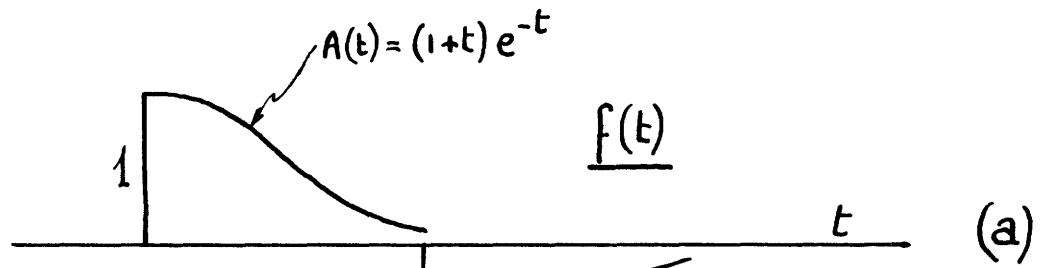


Figure 12

The same type of autocorrelation as the one shown in Fig. 12d would be obtained for pulses of the forms illustrated in Figs. 13 and 14, whose derivatives are positive at the right of the vertical rises.

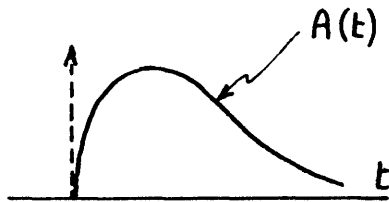


Fig. 13

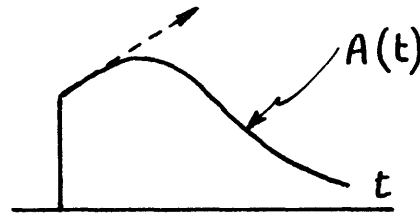


Fig. 14

Some typical results outlined so far in this chapter are summarized in Fig. 15.\*

It should be noticed that if a function  $f(t)$  is turned end for end, the same autocorrelation is obtained: therefore all the pulse shapes studied above may be turned end for end without changing the resulting autocorrelation. We may therefore extend Theorem VI:

Corollary to Theorem VI. If  $f(t)$  contains vertical descents ( $f'(t) = -\infty$ ), immediately followed by a slope which is negative or zero (nonconstant) in the average, the autocorrelation  $\varphi(\tau)$  has negative curvature in the vicinity of  $\tau = 0$ .

---

\* Notice that for the first three rows of Fig. 15, the single column labeled  $-\varphi''$  may be set first under "Assumptions," and the other three columns  $f'$ ,  $f''$ ,  $\varphi$  would appear as "Conclusions." However, for the last row the single information given by  $-\varphi''$  permits one only to derive the corresponding  $\varphi$  curve and to state that  $f'$  becomes infinite.

THEOREM NO.	ASSUMPTIONS		CONCLUSIONS		EXAMPLES OF ELEMENTARY PULSE COMPONENTS OF f(t)	
	f'(t)	f''(t)	-φ'' = φ'f'	φ	SHAPE OF PULSE	PULSE EQUATION
a	REMAINS FINITE	f''(t) REMAINS FINITE				t <sup>2</sup> e <sup>-t</sup>
b	REMAINS FINITE	BECOMES INFINITE				t e <sup>-t</sup>
c	BECOMES INFINITE					e <sup>-t</sup>
d	BECOMES INFINITE, BUT +∞ VALUES ARE FOLLOWED BY ZERO (NON-CONSTANT) OR POSITIVE VALUES IN THE AVERAGE*					(t+1) e <sup>-t</sup>

(\* ) AND -∞ VALUES ARE FOLLOWED BY ZERO (NON-CONSTANT) OR NEGATIVE VALUES IN THE AVERAGE (COROLLARY TO THEOREM VI)

FIGURE 15



## 2. Smooth Time Functions

Let us assume that  $f(t)$  represents an electrical quantity, voltage, current, or charge. Its value is always finite. Its time derivative is also finite. For example, if  $f(t)$  is a current, there is always some inductance in the circuit whose instantaneous energy storage is  $\frac{L}{2} f^2(t)$ ; the rate of change of this energy is  $Lf(t)f'(t)$  and must remain finite in any physical system; therefore  $f'(t)$  is finite. Furthermore, resistance, capacitance, and inductance are always present simultaneously in any physical circuit, and lead to a second-order differential equation for the solution of  $f(t)$ . This equation, therefore, involves  $f(t)$ ,  $f'(t)$ , and  $f''(t)$ ; and since the first two quantities are finite,  $f''(t)$  is also finite.

The same argument applies in the case where  $f(t)$  is a mechanical quantity like velocity, force, or displacement, for which the physical constraints are friction, mass, and stiffness.

Therefore the electromechanical functions  $f(t)$  just considered always yield smooth records: They present no vertical rise [  $f'(t)$  finite ] and no sudden change in slope resulting in angular points [  $f''(t)$  finite ]. The autocorrelation  $\phi(\tau)$  and its second derivative have therefore\* zero slopes at  $\tau = 0$ .

In certain cases, however, this smoothing effect of the energy storage elements is made unappreciable within the range of frequencies involved in the time record of the function  $f(t)$ , whose autocorrelation curve may then approximate the types described above for cases involving

---

\* See Theorem III or Fig. 15a.

infinite derivatives. However, it is convenient to keep in mind that there will always be a finite circle of curvature, however small, enclosed by the autocorrelation curve at  $\tau = 0$ , indicating that  $f'(t)$  and  $f''(t)$ , however large, are still finite. In fact, it will appear in the following pages that the behavior of the autocorrelation in the immediate vicinity of  $\tau = 0$  gives the most valuable information for prediction performance, and needs to be approximated with great accuracy in the Wiener-prediction analysis.

### 3. Jump Time Functions

Many statistical functions give rise to records containing vertical "jumps"; for example, a record of numbers appearing in successive throws of a die would give a random jump function with horizontal steps at integer levels between 1 and 6. Such functions inherently contain infinite derivatives, and their autocorrelation will be of the types described in Fig. 15c and 15d, presenting an angular point at  $\tau = 0$ .

## CHAPTER IV

### The Power Spectrum Function

#### 1. Separation of Conjugate Singularities

It has been pointed out in Chapter II that the autocorrelation should be expressed as a sum of functions whose Fourier Transforms are rational, thus making it possible to split the resulting power spectrum into a product of a finite number of factors. Under such conditions we may write:

$$\Phi(\lambda) = \frac{P_r(\lambda^2)}{Q_s(\lambda^2)}, \quad r < s, \quad (103)$$

where  $P_r$  and  $Q_s$  are polynomials of degree  $r$  and  $s$  in the variable  $\lambda^2$ . The condition  $r < s$  indicates that, for infinite frequencies, the power density must be zero, since the total power of the message is finite.

A first possible expansion of eq. 103 is the following:

$$\Phi(\lambda) = A^2 \frac{(a_1 + j\lambda)(a_2 + j\lambda)\dots(a_r + j\lambda)}{(b_1 + j\lambda)(b_2 + j\lambda)\dots(b_s + j\lambda)} \frac{(a_1 - j\lambda)(a_2 - j\lambda)\dots(a_r - j\lambda)}{(b_1 - j\lambda)(b_2 - j\lambda)\dots(b_s - j\lambda)}, \quad \dots (104)$$

where the complex conjugate pairs of zeros of the polynomials  $P_r$  and  $Q_s$  are in evidence, and  $A^2$  is the positive zero-frequency value of power density. Considering only that part of  $\Phi(\lambda)$  containing singularities lying in the upper half-plane, we have:

$$\Phi^+(\lambda) = A \frac{(a_1 + j\lambda)(a_2 + j\lambda)\dots(a_r + j\lambda)}{(b_1 + j\lambda)(b_2 + j\lambda)\dots(b_s + j\lambda)} \quad (105)$$

and

$$\Psi(t) = \int_{-\infty}^{\infty} \Phi^+(\lambda) e^{j\lambda t} d\lambda, \quad (106)$$

according to the definition (21);  $\Psi(t)$  appears to be the inverse Laplace Transform of a function having poles in the upper half-plane;  $\Psi(t)$  is therefore zero for  $t < 0$ .

An alternate expansion of eq. 103 is:

$$\begin{aligned} \Phi(\lambda) = & \frac{K_1}{(b_1 + j\lambda)} + \frac{K_2}{(b_2 + j\lambda)} + \dots + \frac{K_s}{(b_s + j\lambda)} + \frac{\bar{K}_1}{(b_1 - j\lambda)} + \frac{\bar{K}_2}{(b_2 - j\lambda)} \\ & + \dots + \frac{\bar{K}_s}{(b_s - j\lambda)} \end{aligned} \quad (107)$$

where the constants  $\bar{K}$  are conjugate of the respective  $K$ 's. Considering only poles in the upper half-plane, we have:

$$\Phi_p(\lambda) = \frac{K_1}{(b_1 + j\lambda)} + \frac{K_2}{(b_2 + j\lambda)} + \dots + \frac{K_s}{(b_s + j\lambda)} \quad (108)$$

and

$$\varphi_p(\tau) = \int_{-\infty}^{\infty} \Phi_p(\lambda) e^{j\lambda\tau} d\lambda, \quad (109)$$

where  $\varphi_p(\tau)$  is defined as the inverse Laplace Transform of a function having poles in the upper half-plane, and is therefore zero for  $\tau < 0$ .

From eq. 109 we may write:

$$\Phi_p(\lambda) = \frac{1}{2\pi} \int_0^{\infty} \varphi_p(\tau) e^{-j\lambda\tau} d\tau, \quad (110)$$

$$\overline{\Phi_p(\lambda)} = \frac{1}{2\pi} \int_{-\infty}^0 \varphi_p(-\tau) e^{-j\lambda\tau} d\tau, \quad (111)$$

where the bar indicates "conjugate value of." Since the functions  $\varphi_p(\tau)$  and  $\varphi_p(-\tau)$  do not overlap, we may add eq. 110 and 111 as follows, recalling that  $\Phi_p + \overline{\Phi_p} = \Phi$ , from eqs. 107 and 108:

$$\Phi(\lambda) = \frac{1}{2\pi} \int_{-\infty}^{\infty} \left[ \varphi_p(\tau) + \varphi_p(-\tau) \right] e^{-j\lambda\tau} d\tau. \quad (112)$$

From eq. 19 and 112, it appears that  $\varphi_p(\tau)$  is that portion of the autocorrelation function  $\varphi(\tau)$ , lying to the right of  $\tau = 0$ .

It should be noticed that  $\Phi^+(\lambda)$  and  $\Phi_p(\lambda)$  have the same poles, and their transforms  $\Psi(t)$  and  $\varphi_p(\tau)$  are therefore sums of exponentials in equal number, having respectively the same time constants.

## 2. Differentiation

Integration by parts of eq. 110 yields:

$$2\pi \Phi_p(\lambda) = -\frac{1}{j\lambda} \varphi_p(\tau) e^{-j\lambda\tau} \Big|_0^{\infty} + \frac{1}{j\lambda} \int_0^{\infty} \varphi_p'(\tau) e^{-j\lambda\tau} d\tau.$$

Therefore:

$$\frac{1}{2\pi} \int_0^{\infty} \varphi_p'(\tau) e^{-j\lambda\tau} d\tau = j\lambda \Phi_p(\lambda) - \frac{\varphi_p(0+)}{2\pi}. \quad (113)$$

Integration by parts of eq. 111 yields:

$$2\pi \overline{\Phi_p(\lambda)} = -\frac{1}{j\lambda} \varphi_p(-\tau) e^{-j\lambda\tau} \Big|_{-\infty}^0 + \frac{1}{j\lambda} \int_{-\infty}^0 \varphi_p'(-\tau) e^{-j\lambda\tau} d\tau.$$

Therefore:

$$\frac{1}{2\pi} \int_{-\infty}^0 \varphi_p'(-\tau) e^{-j\lambda\tau} d\tau = j\lambda \overline{\Phi_p}(\lambda) + \frac{\varphi_p(0-)}{2\pi} . \quad (114)$$

Recalling that

$$\varphi_p(0+) = \varphi_p(0-) = \varphi(0) , \quad (115)$$

addition of eq. 113 and 114 gives:\*

$$\frac{1}{2\pi} \int_{-\infty}^{\infty} \varphi'(\tau) e^{-j\omega\tau} d\tau = j\omega \Phi(\omega) . \quad (116)$$

Repetition of the differentiation process on eq. 113 and 114 yields, respectively:

$$\frac{1}{2\pi} \int_0^{\infty} \varphi_p''(\tau) e^{-j\lambda\tau} d\tau = -\lambda^2 \Phi_p(\lambda) - j\lambda \frac{\varphi_p(0+)}{2\pi} - \frac{\varphi_p'(0+)}{2\pi} , \quad (117)$$

and

$$\frac{1}{2\pi} \int_{-\infty}^0 \varphi_p''(-\tau) e^{-j\lambda\tau} d\tau = -\lambda^2 \overline{\Phi_p}(\lambda) + j\lambda \frac{\varphi_p(0-)}{2\pi} + \frac{\varphi_p'(0-)}{2\pi} . \quad (118)$$

By eq. 115, and also recalling that

$$\varphi_p'(0+) = -\varphi_p'(0-) , \quad ** \quad (119)$$

addition of eq. 117 and 118 gives:

\* Equations 113 and 114 hold, respectively, for  $\sigma < 0$  and  $\sigma > 0$ ; the sum holds for  $\sigma = 0$ , or  $\lambda = \omega$ .

\*\* See eq. 80.

$$\frac{1}{2\pi} \int_{-\infty}^{\infty} \varphi''(\tau) e^{-j\omega\tau} d\tau = -\omega^2 \Phi(\omega) - \frac{\varphi'(0+)}{\pi}. \quad (120)$$

It should be noticed that the process leading to eq. 120 avoids the value of  $\varphi''$  at  $\tau = 0$ , and should preferably be written:

$$\frac{1}{2\pi} \left[ \int_{-\infty}^{0-} + \int_{0+}^{\infty} \right] \varphi''(\tau) e^{-j\omega\tau} d\tau = -\omega^2 \Phi(\omega) - \frac{\varphi'(0+)}{\pi}; \quad (121)$$

therefore the point at infinity that appears in  $\varphi''(0)$  when  $f'(t)$  becomes infinite\* is excluded from the integration.\*\* Under such conditions, the theorem on Laplace Transforms, stating that integrals (117) and (118) become zero for  $\lambda \rightarrow \infty$ , applies to integral (120), when  $\omega \rightarrow \infty$ . Therefore:

$$\lim_{\omega \rightarrow \infty} \omega^2 \Phi(\omega) = -\frac{\varphi'(0+)}{\pi} \quad (122)$$

One also finds:†

$$\lim_{\omega \rightarrow \infty} \omega^2 \left[ \omega^2 \Phi(\omega) + \frac{\varphi'(0+)}{\pi} \right] = \frac{\varphi'''(0+)}{\pi}. \quad (123)$$

\* See Chap. III.

\*\* Under such conditions, the inverse transform of eq. 120 reads:

$$-\varphi''(\tau) = \int_{-\infty}^{\infty} \left[ \omega^2 \Phi(\omega) + \frac{\varphi'(0+)}{\pi} \right] e^{j\omega\tau} d\omega, \quad \text{for } \tau \neq 0.$$

† Actually, a sequence of expressions of the same kind may be derived, analogous to (122) and (123). They are seen to relate the behavior of the autocorrelation function around  $\tau = 0$ , to the behavior of the power spectrum at  $\omega = \infty$ . The practical consequences of this correspondence will be discussed in Chap. VI.

Various cases may arise, according to the excess of denominator degree in expression (103) for the power spectrum.

(a)  $s = r + 1$  . For the variable  $\omega$  (or  $\lambda$ ) , the denominator degree exceeds by 2 the numerator degree [for example:  $\Phi(\omega) = \frac{1 + \omega^2}{1 + \omega^4}$ ]. Then eq 122 gives a finite value for initial slope of autocorrelation. From the discussion in the last chapter, this case represents a signal whose derivative becomes infinite (see Fig. 15c and 15d).

(b)  $s = r + 2$  . For example,  $\Phi(\omega) = \frac{1}{(1 + \omega^2)^2}$  . Equation 122 shows that the initial slope of the autocorrelation is zero; substituting this value in eq 123 gives a finite value of slope for  $-\varphi'' = \varphi_{f'f'}$ . This case represents a signal whose first derivative remains finite, but whose second derivative becomes infinite (see Fig. 15b).

(c)  $s = r + 3$  . For example,  $\Phi(\omega) = \frac{1 + \omega^2}{1 + \omega^8}$  . Equations 122 and 123 yield  $\varphi'(0+) = \varphi'''(0+) = 0$  . Both first and second derivatives of the signal remain finite in this case (see Fig. 15a).

It should be noticed that if all derivatives of the signal remain finite, yielding  $\varphi^{(2n+1)}(0+) = 0$  for all integer  $n$  , a rational expression for  $\Phi(\omega)$  could not satisfy all successive equations of the types (122) and (123): Soon, the increasing powers of  $\omega^2$  multiplying the successive equations would give a finite value for  $\varphi^{(2n+1)}(0+)$  . An exponential expression for  $\Phi(\omega)$  avoids this difficulty, but is not adequate for factorization purposes. In practice, however, if the signal  $f(t)$  represents some electromechanical function, very high-order



derivatives are not bound to remain finite,\* and a rational expression for  $\Phi(\omega)$  may apply, provided the denominator degree is sufficiently large. Each additional finite derivative contributes an additional degree in  $\omega^2$  in the denominator of  $\Phi(\omega)$ .

---

\* Theoretically, the nonlinearity of lumped parameters in a physical system results in differential equations involving all derivatives of the signal. Practically, coefficients associated with high-order derivatives are negligible, and corresponding derivatives may become very large.

## CHAPTER V

### A Study of Prediction Error in Relation to Signal and Autocorrelation Behavior

#### 1. The Unit-Transfer-Error Curve

An ideal predictor operating on an input function  $f(t)$  should yield an output  $f(t + \alpha)$ , for a prediction time  $\alpha$ . It is precisely to this perfect output that the actual response  $f_o(t)$  of the predictor is compared in computing the "mean-square error" of prediction:

$$\epsilon = \lim_{T \rightarrow \infty} \frac{1}{2T} \int_{-T}^T [f_o(t) - f(t + \alpha)]^2 dt . \quad (124)$$

If now the predictor system is removed and replaced by a direct connection between input and output terminals (Fig. 16), the new "output" merely reproduces the input  $f(t)$ ,

with no attempt to predict values of  $f(t + \alpha)$ . Obviously, if a predictor system is any good, its output  $f_o(t)$  must do better than  $f(t)$  in approximating  $f(t + \alpha)$ . Using the direct connection in place of the predictor systematically introduces a "prediction" error

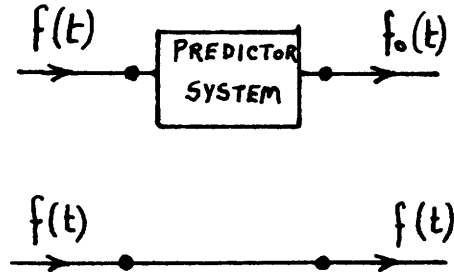


Fig. 16

$$\epsilon_u = \lim_{T \rightarrow \infty} \frac{1}{2T} \int_{-T}^T [f(t) - f(t + \alpha)]^2 dt , \quad (125)$$

which should prove appreciably larger than the error (124) computed

for the predictor. Expression (125) may be called the "unit-transfer-error." It is the mean-square error of prediction obtained with a transfer function equal to unity. Expanding eq. 125 yields:

$$\begin{aligned} \epsilon_u &= \lim_{T \rightarrow \infty} \frac{1}{2T} \int_{-T}^T f^2(t) dt + \lim_{T \rightarrow \infty} \frac{1}{2T} \int_{-T}^T f^2(t + \alpha) dt \\ &\quad - 2 \lim_{T \rightarrow \infty} \frac{1}{2T} \int_{-T}^T f(t) f(t + \alpha) dt . \end{aligned}$$

If  $f(t)$  is in statistical equilibrium, the first two integrals are identical.\* Therefore, by definition of autocorrelation, we have:

$$\epsilon_u = 2 \left[ \varphi(0) - \varphi(\alpha) \right] \quad (126)$$

The curve representing the variation of this error with  $\alpha$  is the mirror image, about an axis of ordinate  $\varphi(0)$ , of twice the autocorrelation curve (Fig. 17).

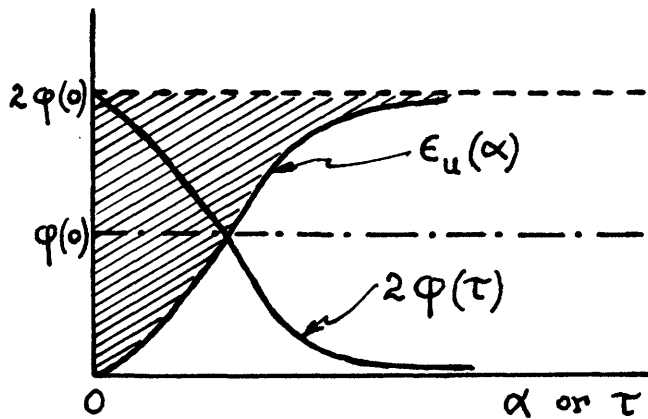


Fig. 17

---

\* They differ only in the origin of time about which the average of  $f^2$  is computed.

If a predictor system is any better than the direct connection, its error curve must always lie in the region below the  $\epsilon_u$  curve, as indicated in Fig. 17.

## 2. The Zero-Transfer-Error Curve

If the predictor system is removed and no connection is made between input and output terminals, the transfer function becomes zero. Again, the actual predictor output  $f_o(t)$  should do better, in approximating  $f(t + \alpha)$ , than an output  $f_o(t) = 0$ . Therefore the error (124) computed for the predictor must be smaller than

$$\epsilon_z = \lim_{T \rightarrow \infty} \frac{1}{2T} \int_{-T}^T f^2(t + \alpha) dt = \varphi(0) . \quad (127)$$

Expression (127) may be called the "zero-transfer-error" and is represented, as a function of  $\alpha$ , by a horizontal line  $\epsilon_z$  of ordinate  $\varphi(0)$ . The error  $\epsilon$  of the predictor system, as a function of  $\alpha$ , must now lie both below the horizontal line  $\epsilon_z$  and below the curve  $\epsilon_u$  drawn in Fig. 17. From Fig. 18 it is recognized that within the

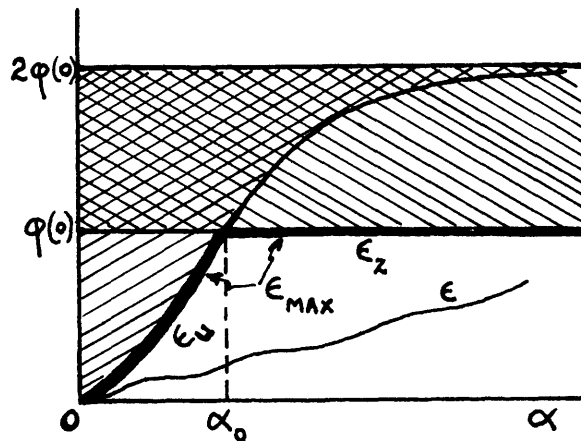


Fig. 18

range  $0 < \alpha < \alpha_0$ ,  $\epsilon_u$  represents the upper limit of the error  $\epsilon$ , and for larger prediction ranges the upper limit is represented by  $\epsilon_z$ . Physically this means that between 0 and  $\alpha_0$ , a convenient standard of comparison for prediction performance is given by the performance of the unit transfer function; above  $\alpha_0$ , a more significant standard of comparison is afforded by the zero transfer function. The composite boundary of prediction error may be called the "maximum" prediction error  $\epsilon_{\max}$ .

### 3. Behavior of the Wiener Prediction Error for Large $\alpha$

Equation 21 gives for  $\alpha = 0$ :

$$\psi(t) = \int_{-\infty}^{\infty} \Phi^+(w) e^{jw t} dw . \quad (128)$$

This expression shows that  $\Phi^+(w)$  is the Fourier Transform of  $\psi(t)$ . Applying Parseval's theorem and noticing that  $\Phi^-(w)$  is the conjugate of  $\Phi^+(w)$ , we have:

$$\int_{-\infty}^{\infty} \Phi^-(w) \Phi^+(w) e^{jw \tau} dw = \frac{1}{2\pi} \int_{-\infty}^{\infty} \psi(t) \psi(t + \tau) dt . \quad (129)$$

By eq. 19 and 18, the first member is

$$\int_{-\infty}^{\infty} \Phi(w) e^{jw \tau} dw = \varphi(\tau) ,$$

and in the second member, the lower limit of integration may be replaced by zero, since  $\psi(t) = 0$  for  $t < 0$ .\*

---

\* See p.52.

Therefore:

$$\varphi(\tau) = \frac{1}{2\pi} \int_0^{\infty} \Psi(t) \Psi(t + \tau) dt . \quad (130)$$

Now eq.23 giving the Wiener prediction error as a function of prediction time  $\alpha$  is rewritten below:

$$\varepsilon_{\min} = \frac{1}{2\pi} \int_0^{\alpha} \Psi^2(t) dt . \quad (131)$$

This expression shows that  $\varepsilon_{\min}$  increases monotonically with increasing  $\alpha$ , since the integrand is always positive. Comparison of eq.130 and 131 shows that when  $\alpha \rightarrow \infty$ ,  $\varepsilon_{\min}$  increases to a maximum value

$$\lim_{\alpha \rightarrow \infty} \varepsilon_{\min} = \varphi(0) .$$

Therefore  $\varepsilon_{\min}$  is asymptotic to  $\varepsilon_z$ , as shown in Fig. 19.

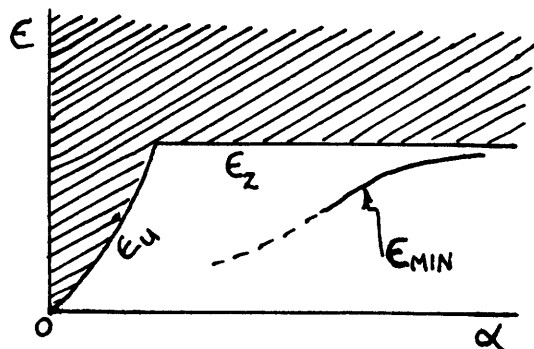


Fig. 19

#### 4. Behavior of the Wiener Prediction Error for Small $\alpha$

The minimum error of prediction starts with the value zero at  $\alpha = 0$ . A significant measure of the Wiener predictor performance

is the rate of increase of the error when the prediction time is increased from zero. Comparison of this rate of increase with that of the unit-transfer-error gives a valuable information on the performance of the Wiener predictor. From eq. 131 we have:

$$\frac{d \varepsilon_{\min}}{d \alpha} = \varepsilon'_{\min} = \frac{1}{2\pi} \Psi^2(\alpha) . \quad (133)$$

For  $\alpha = 0$  :

$$\varepsilon'_{\min}(0) = \frac{1}{2\pi} \Psi^2(0) . \quad (134)$$

From eq. 126 we have:

$$\frac{d \varepsilon_u}{d \alpha} = \varepsilon'_u = -2 \varphi'(\alpha) . \quad (135)$$

According to eq. 130 we have:

$$\varphi(\alpha) = \frac{1}{2\pi} \int_0^{\infty} \Psi(t) \Psi(t + \alpha) dt , \quad (136)$$

$$\frac{d \varphi}{d \alpha} = \varphi'(\alpha) = \frac{1}{2\pi} \int_0^{\infty} \Psi(t) \frac{d}{d \alpha} [\Psi(t + \alpha)] dt , \quad (137)$$

$$\varphi'(\alpha) = \frac{1}{2\pi} \int_0^{\infty} \Psi(t) \frac{d}{dt} [\Psi(t + \alpha)] dt , \quad (138)$$

$$\varphi'(\alpha) = \frac{1}{2\pi} \int_0^{\infty} \Psi(t) \Psi'(t + \alpha) dt . \quad (139)$$

For  $\alpha = 0$  , eq. 139 becomes:

$$\varphi'(0) = \frac{1}{2\pi} \int_0^{\infty} \Psi(t) \Psi'(t) dt , \quad (140)$$

$$\varphi'(0) = \frac{1}{4\pi} \int_0^{\infty} \frac{d}{dt} [\Psi^2(t)] dt, \quad (141)$$

$$\varphi'(0) = \frac{1}{4\pi} [\Psi^2(\infty) - \Psi^2(0)]. \quad (142)$$

But  $\Psi^2(\infty) = 0$ , since integral (131) converges for  $\alpha = \infty$ . Therefore:

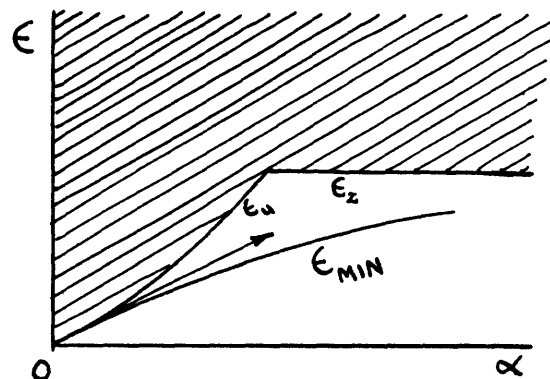
$$\varphi'(0) = -\frac{1}{4\pi} \Psi^2(0). \quad (143)$$

Substituting in eq. 135 gives:

$$\varepsilon'_u(0) = \frac{1}{2\pi} \Psi^2(0). \quad (144)$$

Comparison of eq. 134 and 144 shows that at  $\alpha = 0$ , the rate of change of the Wiener error is the same as the rate of change of the error obtained with a unit transfer function.\* The curves  $\varepsilon_u$  and  $\varepsilon_{\min}$  are tangent at their starting point

(Fig. 20), and give practically the same values of error for small prediction times. However, the  $\varepsilon_{\min}$  curve cannot cross above the  $\varepsilon_u$  curve, since  $\varepsilon_{\min}$  is the minimum theoretical error.



The above result is of fundamental practical importance. Since

Fig. 20

\* If  $\Psi(0) = 0$ , making both "rates of change" equal to zero, a more sensitive comparison of errors must be used: Comparison of the higher-order derivatives will be seen to be adequate for this purpose.



the  $\epsilon_u$  curve was obtained as the mirror image of the autocorrelation curve (after doubling the ordinates of the latter), it appears that the slope of the autocorrelation curve at  $\tau = 0+$  must be known and approximated with great accuracy if we want to prevent the predictor obtained by Wiener's method from yielding a larger error than would be obtained with a unit transfer function (Fig. 21). In particular, the functional approximation to the experimental autocorrelation,

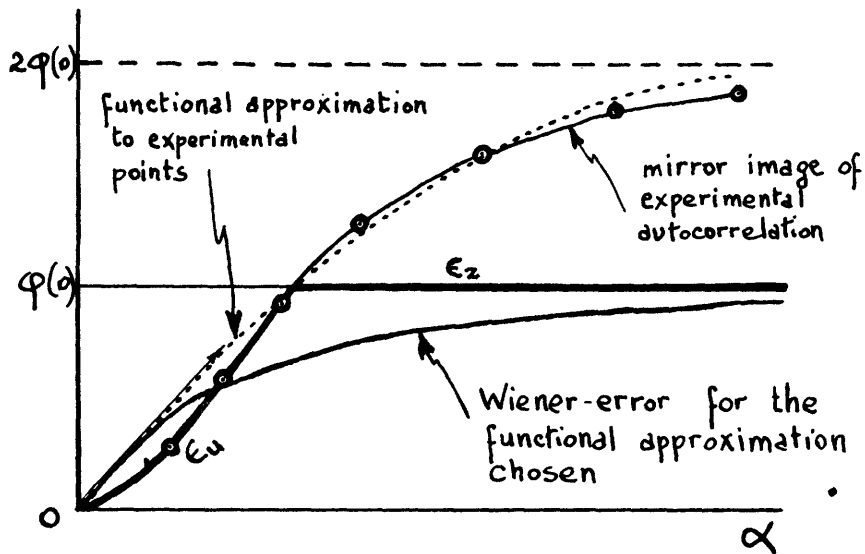


Fig. 21

obtained by an expansion with normal and orthogonal functions, may very well give a curve that apparently follows the experimental points in the average, but gives an incorrect slope at  $\tau = 0$ . This is true of Fig. 4, in which the initial slope of the orthonormal approximating curve (dotted lines) is larger than the slope obtained from the experimental points. As a matter of fact, the autocorrelation of most physical functions\* has zero slope at  $\tau = 0$ , thereby making the  $\epsilon_u$  and  $\epsilon_{\min}$

\* See Chap. III, Section 2.

curves tangent to the  $\alpha$ -axis. However small the range in which the autocorrelation curve is flat around  $\tau = 0$ , this character must be accurately reproduced in the functional approximation, if one wants the Wiener error to increase slowly from the  $\alpha$ -axis for increasing  $\alpha$  (Fig. 22). The importance of reproducing the zero initial slope of the autocorrelation curve is also appreciated from the following additional feature of the  $\epsilon_{\min}$  curve obtained in this case: The  $\epsilon_u$  curve has, at  $\alpha = 0$ , a radius of curvature reducing to  $R = \frac{1}{-2\phi''(0)}$ , a positive quantity\*\* resulting in an upward curvature for  $\epsilon_u$ ; but the radius of curvature of the  $\epsilon_{\min}$  curve is, by eq. 133 and 143,  $R = \frac{\pi}{\Psi(0)\Psi'(0)} = \infty$ . This means that when  $\phi'(0) = 0$ , the Wiener error curve is very flat around  $\alpha = 0$ , its tangency with the  $\alpha$ -axis being of high order: Prediction error remains very small for small ranges of prediction time, and good predictor performance is obtained in these ranges.

It is possible to show that the flatness of the  $\epsilon_{\min}$  curve is improved when the signal has finite derivatives of increasing orders. One first recalls that "flatness" is measured by the number of successive zero derivatives of the  $\epsilon_{\min}$  curve.+ For

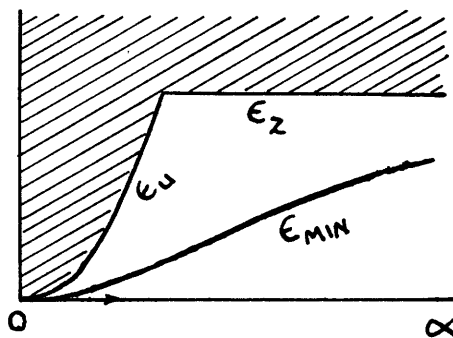


Fig. 22

\* See eq. 100 and 135.

\*\* See Fig. 15a and 15b, corresponding to the case  $\phi'(0) = 0$  here considered.

+ See footnote, next page.

example, from eq. 133,

$$\epsilon_{\min}''(0) = \frac{1}{\pi} \Psi(0) \Psi'(0), \quad (145)$$

$$\epsilon_{\min}'''(0) = \frac{1}{\pi} \Psi(0) \Psi''(0) + \frac{1}{\pi} \Psi'^2(0), \quad (146)$$

and

$$\epsilon_{\min}^{(4)}(0) = \frac{1}{\pi} \Psi(0) \Psi'''(0) + \frac{3}{\pi} \Psi'(0) \Psi''(0) \quad (147)$$

If  $\varphi'(0) = 0$ , corresponding\* to a signal having finite first derivatives, eq 143 gives  $\Psi(0) = 0$ , and therefore  $\epsilon_{\min}''(0) = 0$ , a result which has just been discussed, giving a second-order tangency of  $\epsilon_{\min}$  with the  $\alpha$ -axis. If  $\varphi'''(0)$  is also zero, ( $\varphi''(0) \neq 0$ ), corresponding\*\* to a signal having finite first and second derivatives, one has the following equations: from (139),

$$\varphi'''(\alpha) = \frac{1}{2\pi} \int_0^{\infty} \Psi(t) \Psi'''(t+\alpha) dt; \quad (148)$$

integrating by parts gives:

$$2\pi\varphi'''(\alpha) = \Psi(t) \Psi''(t+\alpha) \Big|_0^{\infty} - \int_0^{\infty} \Psi'(t) \Psi''(t+\alpha) dt;$$

\* Actually, expansion of  $\epsilon_{\min}(\alpha)$  about zero in a Maclaurin series gives:

$$\epsilon_{\min}(\alpha) = \alpha \epsilon_{\min}'(0) + \frac{\alpha^2}{2!} \epsilon_{\min}''(0) + \frac{\alpha^3}{3!} \epsilon_{\min}'''(0) + \dots$$

which shows that if the first (n-1) derivatives are zero at  $\alpha = 0$ ,  $\epsilon_{\min}(\alpha)$  is an infinitesimal quantity of nth order.

\* See Chap. III, Theorem IV.

\*\* See Chap. III, Theorem III, and Fig. 15a.

but  $\psi(\infty) = 0$  and  $\psi(0)$  is still zero, from eq. 143 ; then

$$2\pi \phi'''(0) = - \int_0^{\infty} \psi'(t) \psi''(t) dt ,$$

or

$$0 = - \frac{1}{2} \int_0^{\infty} \frac{d}{dt} [\psi'^2(t)] dt ,$$

or

$$\psi'^2(0) - \psi'^2(\infty) = 0 ,$$

and thence

$$\psi'(0) = 0 ,$$

which, together with  $\psi(0) = 0$  , gives in this case for eq. 146 and 147 :

$$\varepsilon_{\min}'''(0) = \varepsilon_{\min}^{(4)}(0) = 0 ,$$

as well as  $\varepsilon_{\min}''(0) = \varepsilon_{\min}'(0) = 0$  . We see that a fourth-order tangency\* results in this case between the  $\varepsilon_{\min}$  curve and the  $\alpha$ -axis, whereas a simple tangency\*\* still holds for the  $\varepsilon_u$  curve, and prediction is very satisfactory.

The above discussion clearly stresses the importance of approximating all the features of the autocorrelation function at  $\tau = 0$

\* According to the footnote of p. 67, we have in this case  $\varepsilon_{\min}(\alpha) = \frac{\alpha^5}{5!} \varepsilon_{\min}^{(5)}(0) + \dots$  which shows that  $\varepsilon_{\min}$  is a fifth-order infinitesimal quantity.

\*\*  $\varepsilon_u'(0) = \varepsilon_u''(0) = 0$  , since  $\phi'(0) = \phi'''(0) = 0$  ; but  $\phi''(0) \neq 0$  making  $\varepsilon_u''(0) \neq 0$  , and  $\varepsilon_u$  is simply tangent to the  $\alpha$ -axis.

(derivative, radius of curvature, etc.). Figure 23 illustrates the difference in prediction error curves for two autocorrelation functions that differ in shape only in the immediate vicinity of  $\tau = 0$ .

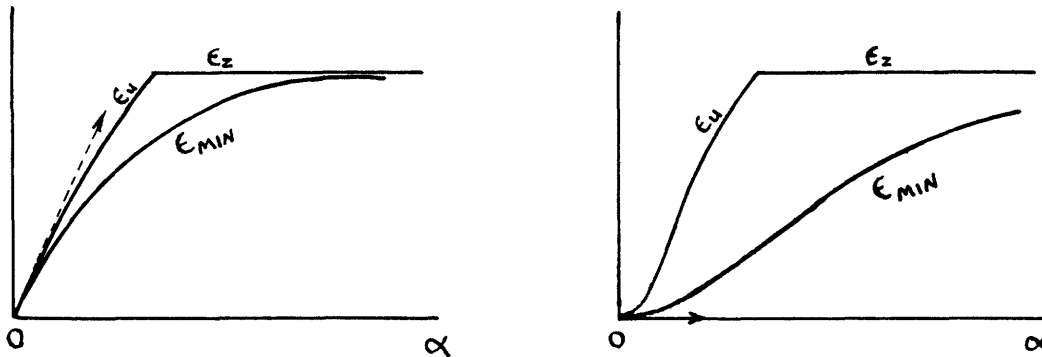


Fig. 23

The physical reasons that make the shape of the  $\epsilon_{\min}$  curve so critically dependent upon the behavior of the autocorrelation around  $\tau = 0$ , are evident from the results of Chapter III, illustrated in Fig. 15. A zero initial slope of autocorrelation corresponds to finite signal derivatives (at least a finite first derivative) and gives a very flat prediction error curve, expressing the fact that future values of the signal do not differ very sharply from present values, within small prediction intervals. A nonzero slope of autocorrelation at  $\tau = 0+$  corresponds to signals having infinite derivatives; the prediction error, as we saw, rises sharply in this case, interpreting the fact that when a vertical jump occurs in the signal, future signal values are difficult to predict.

##### 5. Examples

The following examples of error curves correspond to the typical signal functions studied in Chapter III, for which autocorrelation

curves were computed and sketched (Fig. 7, 8, 9, 12). It is recalled that each case corresponds to a particular behavior of the signal derivatives: accordingly the prediction error will be shown to behave along the patterns anticipated in the preceding sections of the present chapter.

(a) Signal having finite first and second derivatives

The signal chosen is the one illustrated in Fig. 7a. From eq. 82 :

$$\varphi(\tau) = e^{-|\tau|} \left[ \frac{\tau^2}{3} + |\tau| + 1 \right], \quad (149)$$

where  $k$  is made equal to  $4/3$  (average number of pulses per second), in order to normalize the signal to a one-watt power.\* We have:

$$\begin{aligned} \pi \Phi(\omega) &= \frac{1}{3} \int_0^{\infty} \tau^2 e^{-\tau} \cos \omega \tau d\tau + \int_0^{\infty} \tau e^{-\tau} \cos \omega \tau d\tau + \int_0^{\infty} e^{-\tau} \cos \omega \tau d\tau \\ &= \frac{2(1 - 3\omega^2)}{(1 + \omega^2)^3} + \frac{1 - \omega^2}{(1 + \omega^2)^2} + \frac{1}{1 + \omega^2} = \frac{8/3}{(1 + \omega^2)^3}; \end{aligned}$$

$$\Phi^+(\omega) = \frac{2\sqrt{2/\pi}}{\sqrt{3}(1 + j\omega)^3};$$

$$\Psi(t) = \frac{2\sqrt{2/\pi}}{\sqrt{3}} \int_{-\infty}^{\infty} \frac{1}{(1 + jw)^3} e^{jw t} dw = \frac{2\sqrt{2\pi}}{\sqrt{3}} t^2 e^{-t}. \quad (150)$$

The unit-transfer-error curve is, from eq. 149:

$$\varepsilon_u(\alpha) = 2 \left[ \varphi(0) - \varphi(\alpha) \right] = 2 - 2e^{-\alpha} \left[ \frac{\alpha^3}{3} + \alpha + 1 \right], \quad (151)$$

---

\* Assuming the signal to be a voltage across a one-ohm resistor; in that case, eq. 75 gives, for  $n = 0$  :  $f^2(t) =$  average square of the signal  $= \varphi(0) = 1$  watt.

and the Wiener-error curve is, from eq. 150:

$$\varepsilon_{\min}(\alpha) = \frac{1}{2\pi} \int_0^\alpha \Psi^2(t) dt = 1 - \frac{1}{3} e^{-2\alpha} (2\alpha^4 + 4\alpha^3 + 6\alpha^2 + 6\alpha + 3). \quad (152)$$

We have for the unit-transfer-error curve:

$$\varepsilon_u'(0) = 0 ,$$

and

$$\varepsilon_u''(0) = \frac{2}{3} \neq 0 ,$$

indicating that a simple tangency occurs with the  $\alpha$ -axis.

The Wiener-error curve has a derivative  $\varepsilon_{\min}'(\alpha) = \frac{4}{3} \alpha^4 e^{-2\alpha}$ , which yields at  $\alpha = 0$ :

$$\varepsilon_{\min}'(0) = \varepsilon_{\min}''(0) = \varepsilon_{\min}'''(0) = \varepsilon_{\min}^{(4)}(0) = 0 ,$$

and

$$\varepsilon_{\min}^{(5)}(0) = 32 \neq 0 ,$$

indicating that a fourth-order tangency occurs with the  $\alpha$ -axis at  $\alpha = 0$ , for the  $\varepsilon_{\min}$  curve. Curves  $\varepsilon_u$  and  $\varepsilon_{\min}$  are shown in Fig. 24 (solid lines); prediction appears to be very good in this case, for small  $\alpha$ , as expected from the discussion of the preceding section. The prediction time may be chosen between 0 and 1 second, the error remaining very small in this range (less than 5 per cent of the signal power, and less than 18 per cent of the unit-transfer-error).

(b) Signal whose first derivative only remains finite

The signal chosen in this example is the one illustrated in

Fig. 8a. From eq. 86 :

$$\varphi(\tau) = e^{-|\tau|} [|\tau| + 1] , \quad (153)$$

for an average rate of four pulses per second, yielding the same signal power as in the preceding example. We have:

$$\begin{aligned} \pi \Phi(\omega) &= \int_0^{\infty} \tau e^{-\tau} \cos \omega \tau d\tau + \int_0^{\infty} e^{-\tau} \cos \omega \tau d\tau \\ &= \frac{1 - \omega^2}{(1 + \omega^2)^2} + \frac{1}{1 + \omega^2} = \frac{2}{(1 + \omega^2)^2} ; \end{aligned}$$

$$\Phi^+(\omega) = \frac{\sqrt{2/\pi}}{(1 + j\omega)^2} ;$$

$$\Psi(t) = \sqrt{2/\pi} \int_{-\infty}^{\infty} \frac{1}{(1 + j\omega)^2} e^{j\omega t} d\omega = 2\sqrt{2\pi} t e^{-t} . \quad (154)$$

The unit-transfer-error curve is

$$\varepsilon_u(\alpha) = 2 - 2e^{-\alpha}(\alpha + 1) , \quad (155)$$

and the Wiener-error curve is

$$\varepsilon_{\min}(\alpha) = \frac{1}{2\pi} \int_0^{\alpha} 8\pi t^2 e^{-2t} dt \doteq 1 - e^{-2\alpha}(2\alpha^2 + 2\alpha + 1) . \quad (156)$$

We have for the unit-transfer-error curve:

$$\varepsilon_u'(0) = 0 ,$$

and

$$\varepsilon_u''(0) = 2 \neq 0 ,$$

showing that again a simple tangency occurs with the  $\alpha$ -axis.

The Wiener-error curve has a derivative  $\varepsilon_{\min}'(\alpha) = 4\alpha^2 e^{-2\alpha}$ , yielding at  $\alpha = 0$  :



$$\varepsilon'_{\min}(0) = \varepsilon''_{\min}(0) = 0 ,$$

and

$$\varepsilon'''_{\min}(0) = 8 \neq 0 ,$$

which proves that  $\varepsilon_{\min}$  has in this case a second-order tangency with the  $\alpha$ -axis at  $\alpha = 0$  : This result agrees with the discussion of the preceding section of this chapter. Curves of  $\varepsilon_u$  and  $\varepsilon_{\min}$  are shown in Fig. 24 (dashed lines): They indicate that prediction is satisfactory when  $\alpha$  is chosen between 0 and 0.5 . Prediction error is smaller than 8 per cent of the signal power in this range and represents less than 45 per cent of the unit-transfer-error, proving the advantage of using the Wiener transfer function.

- (c) Signal having vertical rises (infinite first derivatives) followed by a zero (nonconstant) or positive average slope \*

The signal studied in this example is the one shown in Fig. 12a.

From eq. 101 :

$$\varphi(\tau) = e^{-|\tau|} (0.6 |\tau| + 1) , \quad (157)$$

for an average rate of 4/5 pulses per second (normalizing the signal power to unity). We have:

$$\begin{aligned} \pi \Phi(\omega) &= 0.6 \int_0^{\infty} \tau e^{-\tau} \cos \omega \tau d\tau + \int_0^{\infty} e^{-\tau} \cos \omega \tau d\tau \\ &= \frac{0.6(1 - \omega^2)}{(1 + \omega^2)^2} + \frac{1}{1 + \omega^2} = \frac{1.6 + 0.4\omega^2}{(1 + \omega^2)^2} ; \end{aligned}$$

---

\* The signal also has (Corollary to Theorem VI) vertical descents, followed by a zero (nonconstant) or negative average slope.

$$\Phi^+(\omega) = \frac{\sqrt{0.4/\pi} (2 + j\omega)}{(1 + j\omega)^2} = \sqrt{\frac{0.4}{\pi}} \left[ \frac{1}{(1 + j\omega)^2} + \frac{1}{1 + j\omega} \right]$$

$$\Psi(t) = \sqrt{\frac{0.4}{\pi}} \int_{-\infty}^{\infty} \left[ \frac{1}{(1 + j\omega)^2} + \frac{1}{1 + j\omega} \right] e^{j\omega t} d\omega \quad (158)$$

$$= \sqrt{1.6\pi} e^{-t} (t + 1) .$$

The unit-transfer-error curve is

$$\varepsilon_u(\alpha) = 2 - 2e^{-\alpha}(0.6\alpha + 1) , \quad (159)$$

and the Wiener-error curve is

$$\varepsilon_{\min}(\alpha) = \frac{1}{2\pi} \int_0^{\alpha} 1.6\pi e^{-2t} (t^2 + 2t + 1) dt = 1 - 0.4e^{-2\alpha} (\alpha^2 + 3\alpha + 2.5) .$$

..... (160)

In agreement with the general analysis, both curves have at zero the same slope

$$\varepsilon_u'(0) = \varepsilon_{\min}'(0) = 0.8 .$$

The curves are represented in Fig. 24 (dotted lines) and are seen to rise sharply along their common tangent from  $\alpha = 0$ . For a prediction time as small as 0.25 seconds, the error obtained with the Wiener predictor is as high as 20 per cent of the signal power, and is practically as large as would be obtained with a unit transfer function. It appears, as expected from earlier theoretical remarks, that for small prediction time the Wiener system function does not give in this case any better prediction than is given by a direct connection between input and output terminals. For larger prediction times the error of

the Wiener predictor departs from the unit-transfer-error, but represents in those ranges a considerable percentage of the signal power, and prediction is very poor. For example, for  $\alpha = 0.75$ , where the Wiener system function gives a smaller error than the direct connection, that error represents nevertheless 52 per cent of the signal power: One can easily realize that the "predicted" waveform would bear very little resemblance to the input waveform.

(d) Signal having vertical rises (infinite first derivatives) followed by a negative average slope (or constant zero slope)

The signal considered is the one shown in Fig. 9a. From eq. 91:

$$\varphi(\tau) = e^{-|\tau|} \quad (161)$$

for an average rate of two pulses per second (giving a signal power equal to unity). We have:

$$\pi \Phi(\omega) = \int_0^{\infty} e^{-\tau} \cos \omega \tau d\tau = \frac{1}{1 + \omega^2} ;$$

$$\Phi^+(\omega) = \frac{\sqrt{1/\pi}}{1 + j\omega} ;$$

$$\Psi(t) = \sqrt{\frac{1}{\pi}} \int_{-\infty}^{\infty} \frac{1}{1 + j\omega} e^{j\omega t} d\omega = \sqrt{4\pi} e^{-t} . \quad (162)$$

The unit-transfer-error curve is

$$\varepsilon_u(\alpha) = 2 - 2e^{-\alpha} , \quad (163)$$

and the Wiener-error curve is

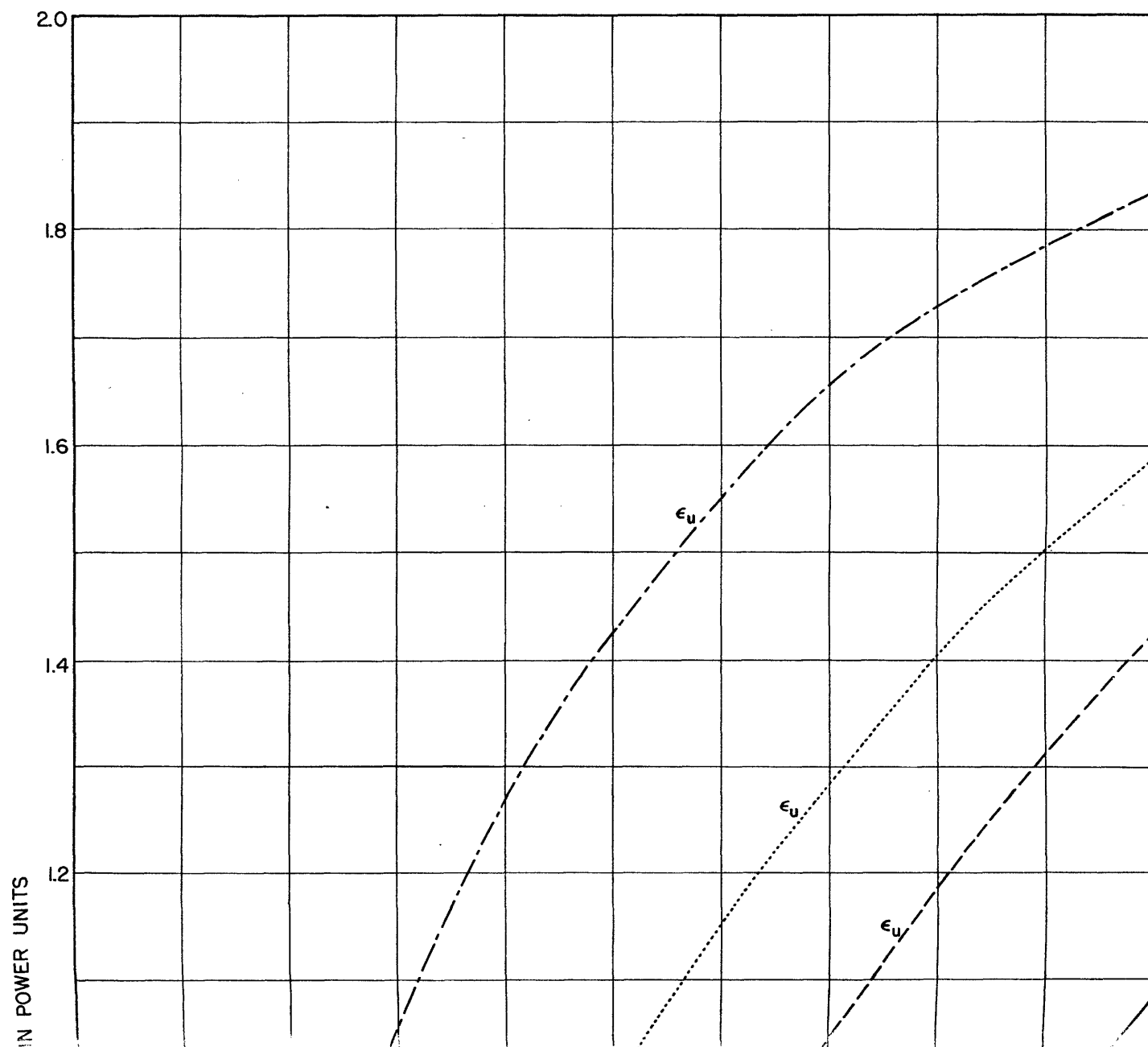
$$\varepsilon_{\min}(\alpha) = \frac{1}{2\pi} \int_0^{\alpha} 4\pi e^{-2t} dt = 1 - e^{-2\alpha} . \quad (164)$$

(a) ————  $\left\{ \begin{array}{l} \epsilon_U = 2 - 2e^{-\alpha} \left( \frac{\alpha^2}{3} + \alpha + 1 \right) \\ \epsilon_{\text{MIN}} = 1 - \frac{e^{-2\alpha}}{3} (2\alpha^4 + 4\alpha^3 + 6\alpha^2 + 6\alpha + 3) \end{array} \right\}$  SIGNAL WHOSE DERIVATIVES  $f'$  AND  $f''$  REMAIN FINITE

(b) - - - - -  $\left\{ \begin{array}{l} \epsilon_U = 2 - 2e^{-\alpha} (\alpha + 1) \\ \epsilon_{\text{MIN}} = 1 - e^{-2\alpha} (2\alpha^2 + 2\alpha + 1) \end{array} \right\}$  SIGNAL WHOSE FIRST DERIVATIVE  $f'$  ONLY REMAINS FINITE

(c) .....  $\left\{ \begin{array}{l} \epsilon_U = 2 - 2e^{-\alpha} (0.6\alpha + 1) \\ \epsilon_{\text{MIN}} = 1 - 0.4e^{-2\alpha} (\alpha^2 + 3\alpha + 2.5) \end{array} \right\}$  SIGNAL WHOSE FIRST DERIVATIVE  $f'$  BECOMES INFINITE

(d) - · - · - ·  $\left\{ \begin{array}{l} \epsilon_U = 2 - 2e^{-\alpha} \\ \epsilon_{\text{MIN}} = 1 - e^{-2\alpha} \end{array} \right\}$



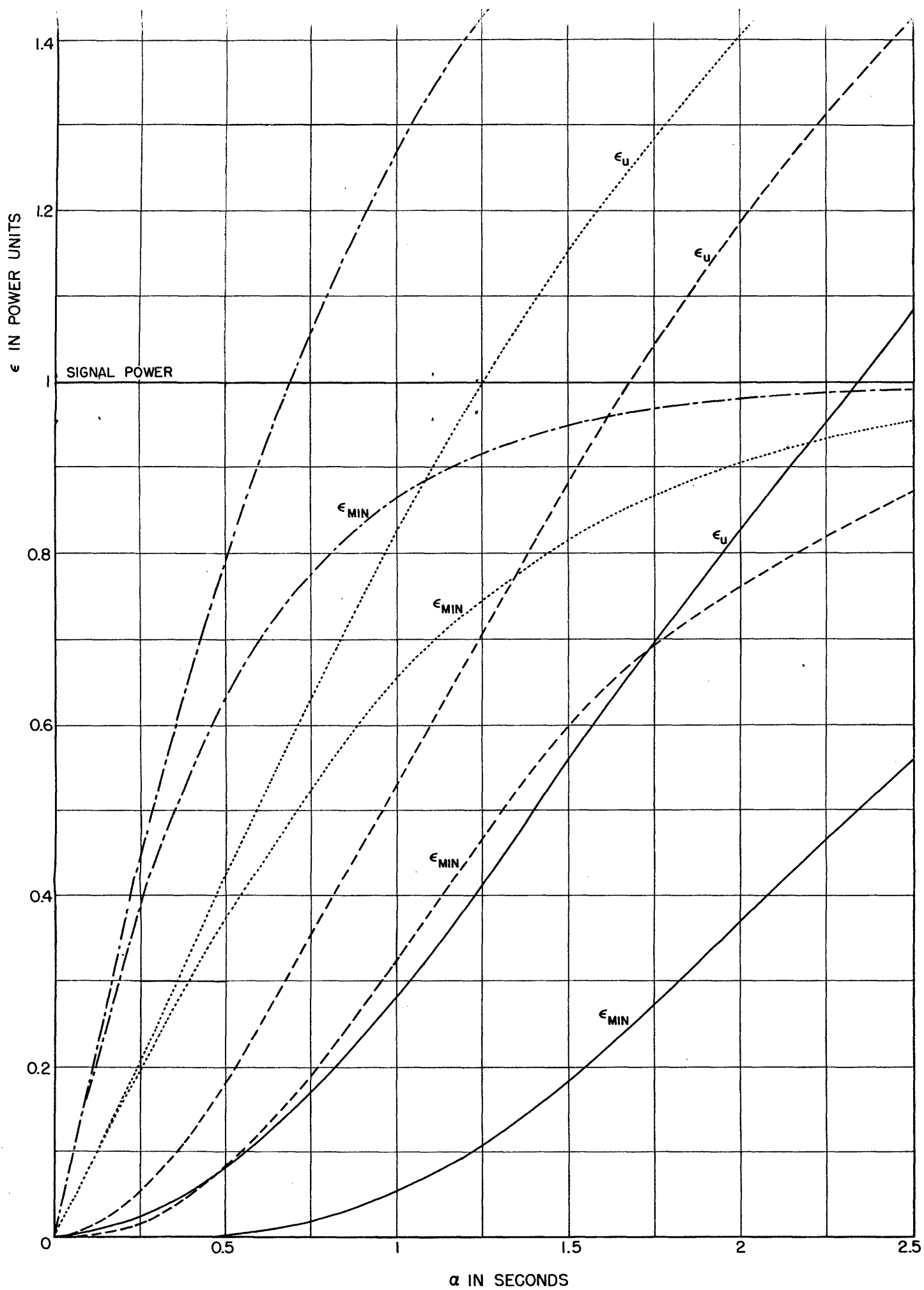


Figure 24.

The common slope condition at  $\alpha = 0$  is verified:

$$\epsilon_u' (0) = \epsilon_{\min}' (0) = 2 \quad .$$

The curves are shown in Fig. 24 (dash-dot lines); it is apparent in this case that there is no prediction that one can speak about. To illustrate the performance of the Wiener system function, we compute its expression

$$H(\lambda) = \frac{1 + j\lambda}{\sqrt{4\pi}} \int_0^{\infty} \sqrt{4\pi} e^{-(t+\alpha)} e^{-j\lambda t} dt = e^{-\alpha}, \quad (165)$$

a constant, independent of  $\lambda$ . This constant, decreasing exponentially when prediction time is increased, merely reduces the ordinates of the input  $f(t)$ . For example, if the random input signal is the one shown in Fig. 25a (which has the same autocorrelation<sup>6</sup> as the signal just considered), the output  $f_o(t)$  results from the graphical construction of Fig. 25b, where it may be compared directly with the actual values of  $f(t + \alpha)$ . It is apparent that however the mean square error has been minimized by the Wiener procedure, the minimum obtained is so large that the output bears no resemblance whatsoever to the curve  $f(t + \alpha)$  which it should approximate.

## 6. The Relative Error in Prediction

In the preceding examples, error curves were computed and plotted for signals normalized to a unit power: Error values could thus be read directly in percentage of signal power. The prediction error for signals having finite derivatives was seen to be small for a certain range of prediction time, but the unit-transfer-error was also small in that range. A new figure of merit is therefore required comparing, for a given type

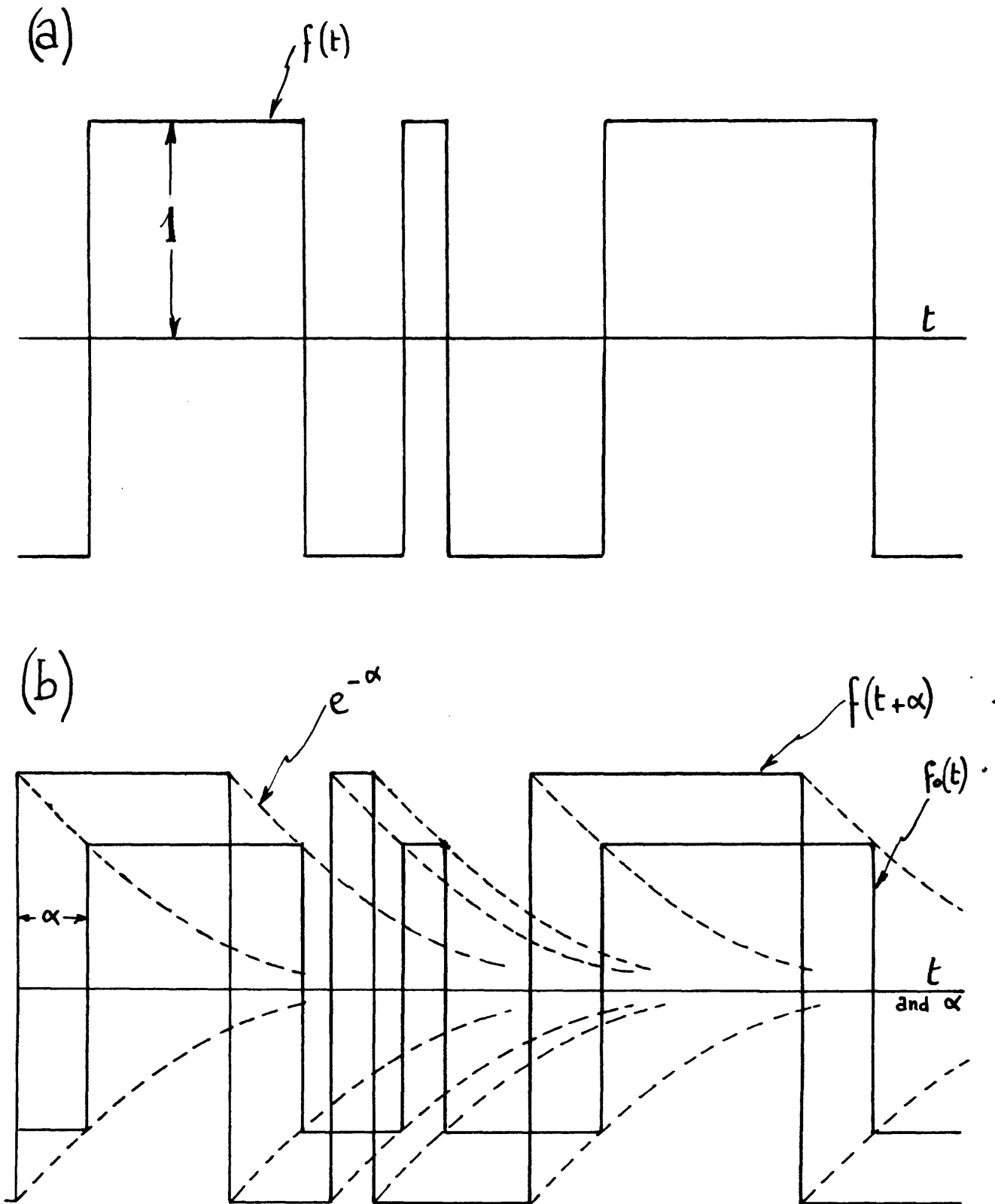


Figure 25

of signal, the advantage of using the Wiener predictor rather than a unit-transfer connection. We may define a relative error:

$$\varepsilon_r = \frac{\varepsilon_{\min}}{\varepsilon_u} \quad (166)$$

However, we have seen that for large prediction time the zero-transfer function gives an error  $\varepsilon_z$  smaller than the error given by a unit-transfer function (Fig. 18). Therefore, after the intersection of the curves  $\varepsilon_u$  and  $\varepsilon_z$ , the significant figure of merit becomes

$$\varepsilon_r = \frac{\varepsilon_{\min}}{\varepsilon_z} = \frac{\varepsilon_{\min}}{\varphi(0)}, \quad (167)$$

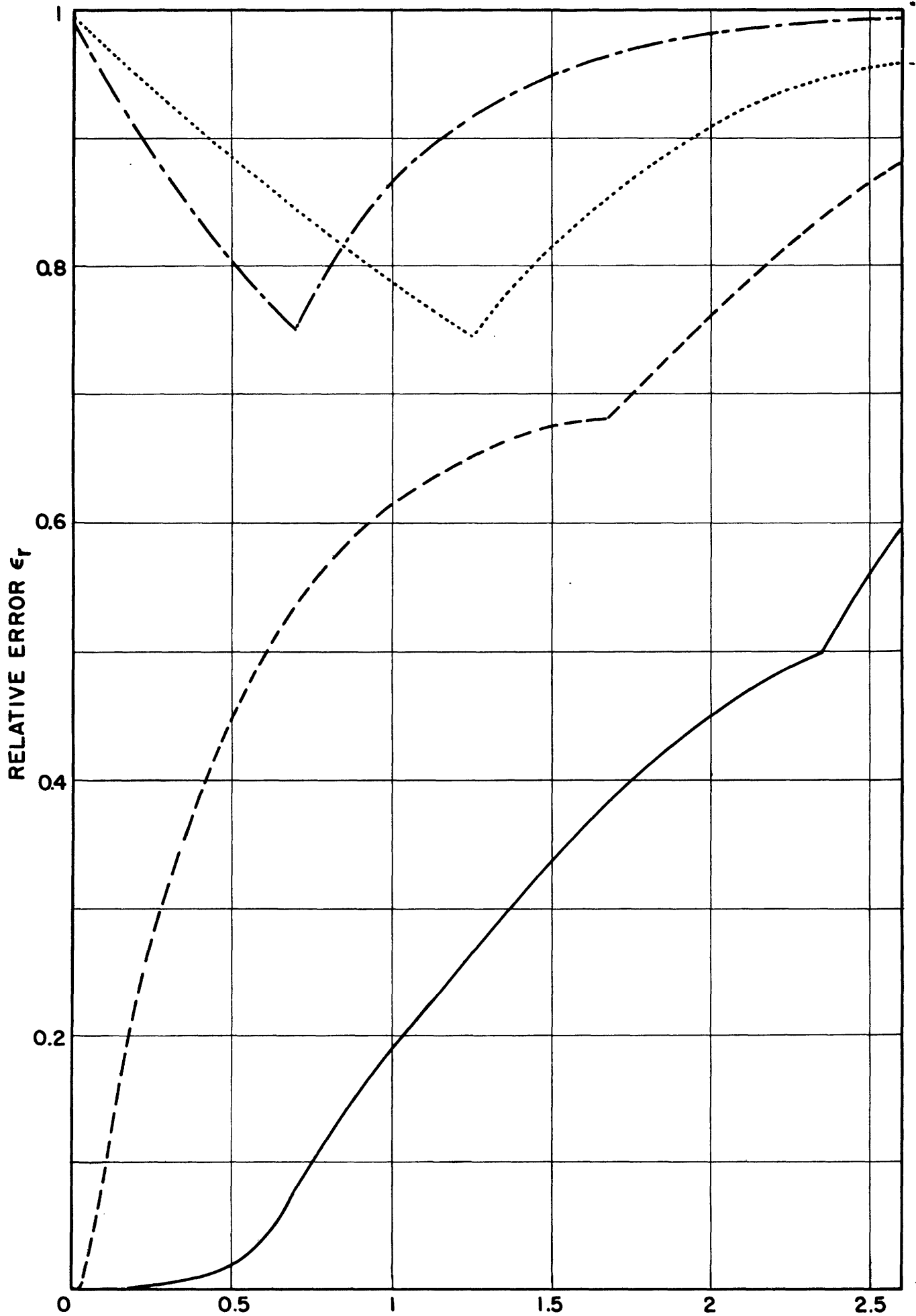
which coincides precisely, for these ranges of  $\alpha$ , with the  $\varepsilon_{\min}$  curves drawn in Fig. 24, normalized to a power  $\varphi(0) = 1$ . Combining eq. 166 and 167 for convenience, we have for the relative error:

$$\varepsilon_r = \frac{\varepsilon_{\min}}{\varepsilon_{\max}}, \quad (168)$$

where  $\varepsilon_{\max}$  is the composite curve shown in Fig. 18. Relative error curves, for each of the four examples of the preceding section, are plotted in Fig. 26. It is easy to show that for the signal (a), having finite first and second derivatives, the function (166) has a third-order tangency with the  $\alpha$ -axis at  $\alpha = 0$  (solid line), whereas the tangency is of first order for the signal (b) whose first derivative only is finite (dashed line). The remaining two curves of relative error, corresponding to signals (c) and (d) having infinite derivatives, start from a value  $\varepsilon_r = 1$  for  $\alpha = 0$ , and remain in the upper region of the graph for all  $\alpha$ , indicating that the Wiener predictor does not perform much better than the direct connection (or the zero transfer



80



$\alpha$  IN SECONDS  
FIGURE 26

for larger  $\alpha$ ) for these types of signals.

The behavior of the relative error curves, illustrated in Fig. 26, in the vicinity of  $\alpha = 0$ , clearly confirms the fact that only those signals are predictable which have at least their first derivative finite.

## CHAPTER VI

### Conclusions

Some of the most significant theoretical results of the preceding chapters are summarized and tabulated in Fig. 27. From a qualitative point of view it may be said that: (a) a signal whose first derivative reaches infinite values is unpredictable; (b) prediction is possible if at least the first derivative of the signal remains finite; and (c) the quality of prediction increases when derivatives of increasing orders of the signal are constrained to remain finite. Assuming that we deal with a predictable signal, whose nature therefore precludes the existence of an infinite first derivative, the fundamental analytical expression of this predictable character lies in the zero initial slope of the autocorrelation of the signal. Reproduction of this slope in the analytical work is the first condition for a successful predictor design. Also, in the immediate vicinity of  $\tau = 0$ , the structure of the autocorrelation curve must be accurately approximated, since it interprets the behavior of the high-order derivatives of the signal, which condition (as we saw) the quality of prediction performance.

The necessity of having accurate data on autocorrelation behavior around  $\tau = 0$  has an important practical consequence. We have seen from eq. 122 and 123 (and others of the like that can be written) that the description of the autocorrelation function at  $\tau = 0$  corresponds to the infinite frequency behavior of the signal power spectrum. It

ASSUMPTION ON SIGNAL DERIVATIVES		BEHAVIOR OF AUTOCORRELATION IN THE VICINITY OF $\tau = 0$ .		DEGREE OF RATIONAL POWER SPECTRUM EXPRESSION $\Phi(\omega) = \frac{P_r(\omega^2)}{Q_d(\omega^2)}$	BEHAVIOR OF PREDICTION-ERROR $\epsilon_{\text{MIN}}$ COMPARED TO UNIT-TRANSFER-ERROR $\epsilon_U$ AND ZERO-TRANSFER-ERROR $\epsilon_Z$		BEHAVIOR OF RELATIVE-ERROR $\epsilon_r = \epsilon_{\text{MIN}}/\epsilon_{\text{MAX}}$		QUALITATIVE COMMENT	EXAMPLES OF ELEMENTARY PULSE COMPONENTS OF THE SIGNAL.	
		AUTOCORR. OF SIGNAL $\phi(\tau)$	AUTOCORR. OF DERIVATIVE SIGNAL $\phi_{\tau\tau} = -\phi''(\tau)$		TYPE OF CURVE	FOR SMALL $\alpha$ $\epsilon_{\text{MIN}} \approx \epsilon_U$ $\epsilon_{\text{MIN}} \approx \epsilon_Z$	TYPE OF CURVE	FOR SMALL $\alpha$ $\epsilon_r \approx$		PULSE SHAPE	PULSE EQUATION
$f'(t)$	$f''(t)$			$S \geq r+3$ (EACH ADDITIONAL DEGREE CORRESPONDS TO AN ADDITIONAL FINITE DERIVATIVE.)				$\frac{k\alpha^3}{k}$	GOOD PREDICTION FOR $\alpha$ RANGING BETWEEN 0 AND AN UPPER LIMIT WHICH INCREASES WITH THE NUMBER OF FINITE DERIVATIVES OF THE SIGNAL		$t^2 e^{-t}$
REMAINS FINITE	REMAINS FINITE			$S = r+2$				$\frac{k\alpha^3}{k}$	UNPREDICTABLE FOR ANY $\alpha$		$te^{-t}$
BECOMES INFINITE	BECOMES INFINITE			$S = r+1$				$\frac{k\alpha^3}{k}$			$e^{-t}$
BECOMES INFINITE, BUT $+\infty$ VALUES ARE FOLLOWED BY ZERO (NON-CONSTANT) OR AVERAGE. POSITIVE VALUES IN THE	BECOMES INFINITE			$S = r+1$				$\frac{k\alpha^3}{k}$		$(t+1)e^{-t}$	

FIGURE 27

is therefore inadequate to take experimental data of power spectrum, since the solution of the prediction problem would require approximating with extreme accuracy the manner in which the power spectrum approaches zero for large  $\omega$ ; moreover, however large the frequency range in which the experiment is performed, the most important data would still lie beyond that range.\* In practice, therefore, the power-spectrum equation, representing the signal statistics in all of Wiener's analytical work, must be derived merely as the Fourier Transform of the autocorrelation curve. The above argument is made clear from inspection of Fig. 28.\*\* All curves are represented only for positive abscissae and must be completed by symmetry about the ordinate axis. The  $g_0(\sigma)$  curves have the general character of autocorrelation functions (except curve 1<sup>+</sup>); they show a variety of forms in the range of the graph, corresponding to the various cases considered in the preceding chapters. The  $G_0(\Omega)$  curves are the normalized Fourier Transforms of the respective  $g_0(\sigma)$  curves; they may be interpreted as the power spectra associated with the corresponding autocorrelation curves  $g(\sigma)$ . It clearly appears that the considerable differences between

---

\* This result stresses the fact that prediction performance is related to the behavior of the high-frequency components of the signal, which are responsible for the steep rises and sharp corners.

\*\* Taken from: "A Case of Linear Pulse Distortion Occurring in Ionospheric Work," by H. Baerwald (Technical Physics of the USSR, Vol. 3, No. 7, p. 7, 1936).

<sup>+</sup> Wiener has shown<sup>1</sup> from the Schwartz inequality that the autocorrelation  $\phi(\tau)$  is smaller (and never equal) for any  $\tau$  than the value it has at  $\tau = 0$ .

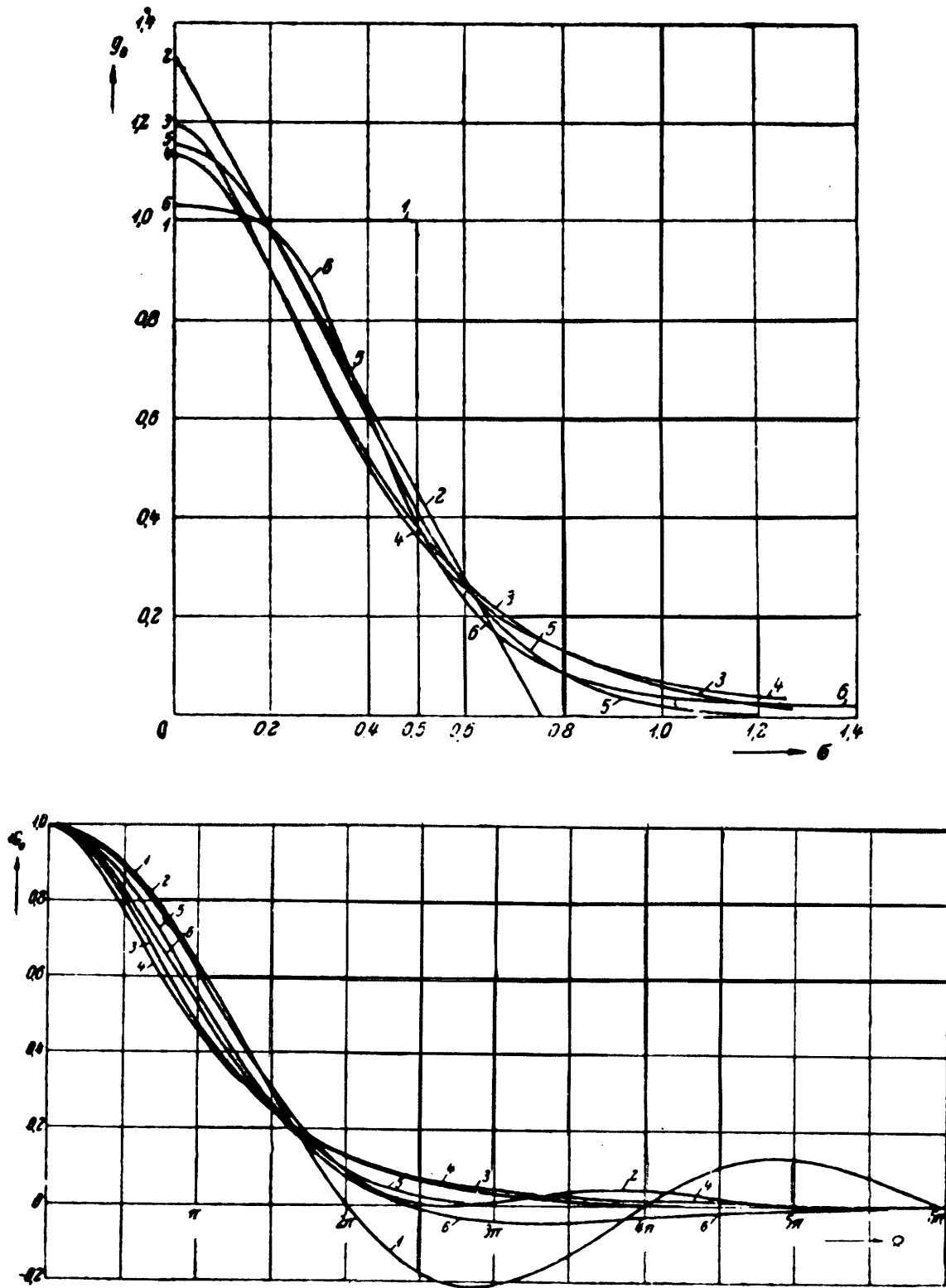


FIGURE 28

the various  $g_0(\sigma)$  curves around  $\sigma = 0$  are greatly reduced in the Fourier Transform curves, which differ mainly in the way they approach their common zero asymptote for large  $\Omega$ . If one has experimental data for a  $G_0(\Omega)$  curve, it becomes impractical to reproduce accurately the important part, which lies in the highest frequency ranges; it is much simpler to obtain experimental data for  $g_0(\sigma)$  in a narrow range around  $\sigma = 0$ , and take the Fourier integral of the corresponding expression.

As far as the trial experiment of Chapter II is concerned, it is now clear that failure of an adequate approximation of autocorrelation behavior around  $\tau = 0$  accounts for the poor performance of the resulting predictor. More experimental points are needed for small values of  $\tau$  than the ones recorded in Fig. 4. Inspection of the signal function of Fig. 1 shows that a zero slope of autocorrelation should result at  $\tau = 0$ , rather than the negative slopes given by expression (51) or (54). Failure to meet the correct slope at zero causes all further analytical steps to follow the pattern of the last two rows of Fig. 27, corresponding to "unpredictable" signals. As a matter of fact, expression (54) used for autocorrelation of the signal of Fig. 1 gave a system function practically reducing to a constant; this result is comparable to the one obtained in eq. 165 for the unpredictable functions studied in Example (d) of the preceding chapter.

New procedures must therefore be used for an adequate fitting of experimental data for the autocorrelation function. For example,

an expression of the form

$$\varphi(\tau) = \varphi_0(\tau) - he^{-a\tau} \cos b\tau, *$$

where  $h$  is chosen very small and  $a$  very large, may account for the zero initial slope of  $\varphi(\tau)$  and its rapid change in the vicinity of  $\tau = 0$ . The term  $\varphi_0(\tau)$  is usually a sum of decreasing exponentials\*\* whose negative contributions to the initial slope may be offset by the positive contribution  $ah$  of the second term, for adequate values of  $a$  and  $h$ . In most cases,  $a$  must be so large that the oscillations produced by  $\cos b\tau$  are completely damped out before the first half-period is over. The parameter  $b$  appears in the second derivative of  $\varphi(\tau)$ , and may be chosen to give the optimum description of slope variation around  $\tau = 0$ .

Dr. Manuel Cerrillo, of the M.I.T. Research Laboratory of Electronics, is developing an orthonormal system of functions which would be particularly convenient for fitting curves having structures of the autocorrelation types.

---

\* Use of the small subtractive term  $he^{-a\tau} \cos b\tau$  in the expression for  $\varphi(\tau)$  was suggested to the author by Dr. Y. W. Lee.

\*\* Making the power spectrum rational.



## APPENDIX I (See Fig. 6)

$\tau$	$\varphi(\tau)$	$\varphi_1(\tau)$	$5.809e^{-\tau}$	$\varphi_2(\tau)$
0	5.849	5.809	5.809	0
0.2	5.276	5.236	4.750	0.486
0.4	4.289	4.249	3.895	0.354
0.6	3.598	3.558	3.188	0.370
0.8	2.810	2.770	2.610	0.160
1.0	2.273	2.233	2.140	0.093
1.2	1.675	1.635	1.750	-0.115
1.4	1.416	1.376	1.435	-0.060
1.6	1.180	1.140	1.175	-0.035
1.8	1.176	1.136	0.960	0.176
2.0	1.098	1.058	0.785	0.273
2.2	0.856	0.816	0.645	0.171
2.4	0.847	0.807	0.529	0.278
2.6	0.809	0.769	0.430	0.339
2.8	0.764	0.724	0.354	0.370
3.0	0.681	0.641	0.290	0.351
3.2	0.603	0.563	0.237	0.326
3.4	0.535	0.495	0.194	0.301
3.6	0.450	0.410	0.157	0.253
3.8	0.425	0.385	0.129	0.256
4.0	0.368	0.328	0.106	0.222
4.2	0.249	0.209	0.087	0.122
4.4	0.267	0.227	0.071	0.156
4.6	0.227	0.187	0.058	0.129

$\varphi(\tau)$  : experimental values (see Fig. 4)

$$\varphi_1(\tau) = \varphi(\tau) - 0.04 \quad (\text{see eq. 31})$$

$$\varphi_2(\tau) = \varphi_1(\tau) - 5.809 e^{-\tau} \quad (\text{see eq. 35})$$

APPENDIX II (See Fig. 4)

A	B	C	D	E	F	G	H	I	J
$\tau$	$e^{-2\tau}$	$\tau^6$	$e^{-8\tau}$	$\tau^2$	$5.809e^{-\tau}$	$59.5\tau^2 e^{-8\tau}$	$0.182\tau^6 e^{-2\tau}$	$\varphi_1(\tau)$	$\varphi(\tau)$
0	1.00000	0	1.00000	0	5.809	0	0	5.809	5.849
0.2	0.67032	0	0.20190	0.04	4.750	0.480	0	5.230	5.270
0.4	0.44933	0.0041	0.04076	0.16	3.895	0.388	0	4.283	4.323
0.6	0.30119	0.0466	0.00823	0.36	3.188	0.176	0.002	3.366	3.406
0.8	0.20190	0.2625	0.00167	0.64	2.610	0.063	0.010	2.683	2.723
1.0	0.13534	1	0.00034	1.00	2.140	0.020	0.025	2.185	2.225
1.5	0.04979	11.38	$6.13 \cdot 10^{-6}$	2.25	1.295	0.001	0.103	1.399	1.439
2.0	0.01832	64	0	4.00	0.785	0	0.213	0.998	1.038
2.5	0.00674	242	0	6.25	0.477	0	0.297	0.774	0.814
3.0	0.00248	730	0	9.00	0.290	0	0.330	0.620	0.660
4.0	0.00034	4080	0	16.00	0.106	0	0.253	0.359	0.399
4.5	0.00012	8400	0	20.25	0.059	0	0.183	0.242	0.282

Functional approximation:

$$\varphi(\tau) = 5.809 e^{-\tau} + 59.5 \tau^2 e^{-8\tau} + 0.182 \tau^6 e^{-2\tau} + 0.04$$

## APPENDIX III

An orthonormal expansion, using Legendre functions, will be computed for the expression

$$\varphi_1(\tau) = 5.809 e^{-\tau} + 59.5 \tau^2 e^{-8\tau} + 0.182 \tau^6 e^{-2\tau} \quad (51)$$

For a three-term approximation, the first three Legendre functions must be used. They are:

$$\begin{aligned} Q_0(\tau) &= \sqrt{p} e^{-p\tau/2} \\ Q_1(\tau) &= \sqrt{3p} e^{-p\tau/2} (2e^{-p\tau} - 1) \\ Q_2(\tau) &= \sqrt{5p} e^{-p\tau/2} (6e^{-2p\tau} - 6e^{-p\tau} + 1) \end{aligned} \quad (51a)$$

The resulting expression for eq. 51 will be:

$$\varphi_1(\tau) = \sum_{n=0}^2 c_n Q_n(\tau) \quad (51b)$$

with

$$c_n = \int_0^{\infty} \varphi_1(\tau) Q_n(\tau) d\tau \quad (51c)$$

$$c_n = 5.809 \underbrace{\int_0^{\infty} e^{-\tau} Q_n(\tau) d\tau}_R + 59.5 \underbrace{\int_0^{\infty} \tau^2 e^{-8\tau} Q_n(\tau) d\tau}_S + 0.182 \underbrace{\int_0^{\infty} \tau^6 e^{-2\tau} Q_n(\tau) d\tau}_T$$

After trial, it has been found that the optimum set of functions (51a) is obtained for

$$p = 0.32$$

$Q_n$  will contain therefore terms of the forms:

$$e^{-0.16\tau} \quad e^{-0.48\tau} \quad e^{-0.8\tau}$$

For  $Q_n = e^{-0.16\tau}$  :

$$R = \int_0^{\infty} e^{-1.16\tau} d\tau = 0.861$$

$$S = \int_0^{\infty} \tau^2 e^{-8.16\tau} d\tau = 0.0037$$

$$T = \int_0^{\infty} \tau^6 e^{-2.16\tau} d\tau = 3.30$$

For  $Q_n = e^{-0.48\tau}$  :

$$R = \int_0^{\infty} e^{-1.48\tau} d\tau = 0.6755$$

$$S = \int_0^{\infty} \tau^2 e^{-8.48\tau} d\tau = 0.00334$$

$$T = \int_0^{\infty} \tau^6 e^{-2.48\tau} d\tau = 1.257$$

For  $Q_n = e^{-0.8\tau}$  :

$$R = \int_0^{\infty} e^{-1.8\tau} d\tau = 0.5555$$

$$S = \int_0^{\infty} \tau^2 e^{-8.8\tau} d\tau = 0.00294$$

$$T = \int_0^{\infty} \tau^6 e^{-2.8\tau} d\tau = 0.5335$$

Using now the complete expressions of  $Q_0$ ,  $Q_1$ , and  $Q_2$ , and developing the corresponding coefficients  $C_0$ ,  $C_1$ , and  $C_2$  according to eq. 51c, we get:

$$C_0 = \sqrt{0.32} (5.809 \times 0.861 + 59.5 \times 0.0037 + 0.182 \times 3.30) = 3.298$$

$$C_1 = \sqrt{0.96} (2 \times 5.809 \times 0.6755 + 2 \times 59.5 \times 0.00334 + 2 \times 0.182 \times 1.257 - \frac{C_0}{\sqrt{0.32}}) = 2.82$$

$$C_2 = \sqrt{1.6} (6 \times 5.809 \times 0.5555 + 6 \times 59.5 \times 0.00294 + 6 \times 0.182 \times 0.5335 - \frac{3C_1}{\sqrt{0.96}} - \frac{2C_0}{\sqrt{0.32}}) = 0.972$$

Finally, from eq 51b, we obtain:

$$\begin{aligned} \varphi_1(\tau) = e^{-0.16\tau} & \left\{ 0.972 \sqrt{1.6} \times 6e^{-0.64\tau} \right. \\ & + (2.82 \sqrt{0.96} \times 2 - 0.972 \sqrt{1.6} \times 6)e^{-0.32\tau} \\ & \left. + (0.972 \sqrt{1.6} + 3.298 \sqrt{0.32} - 2.82 \sqrt{0.96}) \right\} \\ \varphi_1(\tau) = & 7.365 e^{-0.8\tau} - 1.855 e^{-0.48\tau} + 0.332 e^{-0.16\tau} \end{aligned} \quad (54)$$

This is the desired three-term expansion of eq. 51.

The following values of this expansion were computed, and the corresponding curve plotted in Fig. 4 :

$\tau$	$\varphi_1(\tau)$ , eq 54	$\varphi = \varphi_1 + 0.04$
0	5.842	5.882
0.2	4.909	4.949
0.4	4.136	4.176
0.6	3.464	3.504
0.8	2.914	2.954
1.0	2.442	2.482
1.5	1.577	1.617
2.0	1.019	1.059
3.0	0.433	0.473
4.0	0.203	0.243

## APPENDIX IV

Numerical Analysis of  
System Function Performance

The system function, or "transfer" function  $H(\omega)$  obtained by the methods described in this paper, can always be realized by a linear electromechanical system. However, errors are introduced by the physical elements used in the synthesis, and greater accuracy is obtained by computing the theoretical system performance. If  $f_1(t)$  is the input function, for which the optimum  $H(\omega)$  has been obtained by Wiener's method, we may describe the theoretical filter output by

$$(a) \quad f_{01}(t) = \int_0^{\infty} f_1(t - \tau) h(\tau) d\tau ,$$

where

$$(b) \quad h(\tau) = \frac{1}{2\pi} \int_{-\infty}^{\infty} H(\omega) e^{j\omega\tau} d\omega \quad *$$

represents the output for a unit impulse input  $u(\tau)$  .

For the system function given by eq. 62, for example, eq. (b) gives directly:

$$h(\tau) = 0.6476 u(\tau) + 0.01083 e^{-0.189\tau} - 0.0171 e^{-0.392\tau}$$

where  $u(\tau)$  is the unit impulse function. In this case, eq. (a) becomes:

$$(c) \quad f_{01}(t) = 0.6476 f_1(t) + \int_0^{\infty} h_1(\tau) f_1(t - \tau) d\tau ,$$

$$(d) \quad \text{with } h_1(\tau) = 0.01083 e^{-0.189\tau} - 0.0171 e^{-0.392\tau} .$$

---

\* These equations are true for any system function.

The integral appearing in eq. (c) is computed by the same procedure described on pp. 15 and 17 for the autocorrelation function. For the present case, a list of values of  $h_1(\tau)$  is computed, for  $\tau = n \times 0.2$  for example,  $n$  increasing from 0 to a value  $N$ , after which  $h_1(\tau)$  is practically zero. In front of this list, values of  $f_1$  are listed, for decreasing  $t$ , time intervals being of the same magnitude 0.2; if the record covers the range from 0 to  $T_0$ , the first number of this list will be  $f_1(T_0)$ . Now the  $h_1(\tau)$  list is slid along the  $f_1$  list until  $h_1(0)$  is in front of the value  $f_1(t)$  at the time  $t$  for which the "output" given by eq. (c) is sought. As illustrated by the tabulation below, horizontal products represent discrete values of the integrand of eq (c), separated by equal intervals of magnitude 0.2 .

$f_1(T_0)$				
.				
.				
-----				
$f_1(t)$	x	$h_1(0)$	=	$p_0$
$f_1(t - 0.2)$	x	$h_1(0.2)$	=	$p_1$
$f_1(t - 0.4)$	x	$h_1(0.4)$	=	$p_2$
.	.	.		
.	.	.		
.	.	.		
$f_1(t - N \times 0.2)$	x	$h_1(N \times 0.2)$	=	$p_N$
-----				
.		0		
.		0		
.		0		
$f_1(0)$		0		



If values of the integrand are plotted as in Fig. 5, the trapezoidal approximation to the integral of eq. (c) yields:

$$\int_0^{\infty} h_1(\tau) f_1(t - \tau) d\tau \cong 0.2 \left[ \frac{p_0}{2} + p_1 + p_2 + \dots + p_{N-1} + \frac{p_N}{2} \right]$$

The particular case here described by eq. (c) and (d) makes the value of this integral insignificant compared to the term  $0.6476 f_1(t)$  of eq. (c); this result was pointed out on p. 27 of this paper.

However, the computational method described by the tabulation shown above is completely general. The tabulation clearly illustrates the mechanism by which a filter system, described by  $H(\omega)$  or  $h(\tau)$ , operates on the past of the input function, past values of the input contributing to the present output in a way determined by the "weighting factor"  $h(\tau)$ . This factor represents the distribution in the past of the contributions of the input; since it decreases exponentially, we have the obvious result that values of the input function lying in the infinite past have negligible effect upon the present output.

## APPENDIX V

Scheme of Computation for  
Mean Square Prediction Error

For the experiment described in Chapter II, the "predicted" output for a time interval  $\alpha = 0.5$  is given by eq. 63, yielding:

$$f_{01}(t) = f_0(t) + 0.20 = 0.6476 f_1(t) = 0.6476 [f(t) + 0.20] ,$$

or

$$f_0(t) = 0.6476 f(t) - 0.07 ,$$

where  $f_0(t)$  is the "filter" output referred to the co-ordinate axes of the input record of Fig. 4.

In order to determine the mean-square error of prediction, this output has to be compared with the value of the input at the later time  $(t + 0.5)$ . A scheme of tabulation of results is indicated below and the actual value obtained in the summation of the last column is shown.

t	t+0.5	f(t)	0.6476f(t)	f <sub>0</sub> (t)	f(t+0.5)	$ f_0(t) - f(t+0.5) ^2$
48.8	49.3	3.4	2.20	2.13	2.2	0.005
48.6	49.1	1.0	0.65	0.58	4.2	13.10
48.4	48.9	0	0	-0.07	4.1	17.38
.	.	.	.	.	.	.
.	.	.	.	.	.	.
.	.	.	.	.	.	.
27.4	27.9	1.7	1.10	1.03	-1.5	6.40
						<u>318.62</u>

The square-error summation, for the 108 samples of the tabulation, is 318.62. The approximate mean-square error is therefore

$$(a) \quad \epsilon = \frac{318.62}{108} = 2.95 \quad (\text{experimental}) .$$

We must compare this performance with the theoretical one, expressed by eq. 23, which is repeated below:

$$\epsilon_{\min} = \frac{1}{2\pi} \int_0^{\alpha} \Psi^2(t) dt . \quad (23)$$

From eq. 60 we have:

$$\begin{aligned} \Psi^2(t) &= 4\pi^2 \left[ 1.543 e^{-0.8t} - 0.317 e^{-0.48t} + 0.0416 e^{-0.16t} \right]^2 \\ \Psi^2(t) &= 4\pi^2 \left[ 2.38 e^{-1.6t} + 0.01 e^{-0.96t} + 0.00173 e^{-0.32t} \right. \\ &\quad \left. - 0.979 e^{-1.28t} + 0.1285 e^{-0.96t} - 0.0264 e^{-0.64t} \right] \end{aligned}$$

Then eq. 23 reads:

$$\begin{aligned} \epsilon_{\min} &= 2\pi \left[ \frac{2.38}{1.6} (1 - e^{-1.6\alpha}) + \frac{0.1385}{0.96} (1 - e^{-0.96\alpha}) \right. \\ &\quad + \frac{0.00173}{0.32} (1 - e^{-0.32\alpha}) - \frac{0.979}{1.28} (1 - e^{-1.28\alpha}) \\ &\quad \left. - \frac{0.0264}{0.64} (1 - e^{-0.64\alpha}) \right] \end{aligned}$$

For  $\alpha = 0.5$  we get:

$$(b) \quad \epsilon_{\min} = 3.15 \quad (\text{theoretical}) .$$

The experimental value obtained in eq (a) is in good agreement with the theoretical value (b), computed directly from the analytical expression of the autocorrelation function [since  $\Psi(t)$  is uniquely determined by  $\varphi(t)$ ].

#### ACKNOWLEDGMENTS

The author wishes to express his grateful appreciation to Dr. Y. W. Lee for the incentive of his lectures on Wiener's Theory and for his helpful advice; to Mr. T. P. Cheatham for his comments and suggestions; and to the Directors of the Research Laboratory of Electronics and their associates for providing the research facilities.

## BIBLIOGRAPHY

1. N. Wiener, "The Extrapolation, Interpolation and Smoothing of Stationary Time Series," NDRC Report, M.I.T., Feb. 1, 1942.
2. G. I. Taylor, "Diffusion by Continuous Movements," London Math. Soc. Proceedings, Ser. 2, Vol. 20, pp. 196-212, 1920.
3. N. Wiener, "Generalized Harmonic Analysis," Acta Mathematica, Vol. 55, pp. 117-258, 1930.
4. N. Wiener, "The Harmonic Analysis of Irregular Motion," Jour. of Math. and Phys., Vol. 5, pp. 99-121 and 158-189, 1926.
5. G. W. Kenrick, "The Analysis of Irregular Motions With Applications to the Energy-Frequency Spectrum of Static and of Telegraph Signals," Phil. Mag., Ser. 7, Vol. 7, pp. 176-196, 1929.
6. Y. W. Lee, "Theory of Optimum Linear Systems." (Notes dictated at M.I.T., course 6.563 - as yet unpublished)
7. H. M. James, N. B. Nichols, R. S. Phillips, "Theory of Servomechanisms," M.I.T. Radiation Laboratory Series, Vol. 25, Chapters 6-8, 1947 (N.Y., McGraw-Hill Book Company, Inc.).
8. N. Levinson, "A Heuristic Exposition of Wiener's Mathematical Theory of Prediction and Filtering," Jour. of Math. and Phys., Vol. 26, pp. 110-119, 1947.